低電壓超快速聚焦液晶透鏡

碩士研究生：林裕閔　　指導教授：謝漢萍教授
黃乙白副教授

國立交通大學　　光電工程研究所

摘要

手機結合相機功能是近幾年手機發展的主要潮流。現今照相手機多是利用數位變焦以達到變焦的功能，影像品質並不如利用光學變焦。傳統光學變焦是透過設置一透鏡組，利用機械化移動透鏡間距離，控制其等效的焦距長度。然而此法需要足夠的空間容納眾多透鏡，且也有機械性損耗的問題。若要將傳統透鏡組結合至體積輕薄短小的照相手機裡，將面臨很大的挑戰。

本研究提出一種可調焦液晶透鏡，其特色是短聚焦反應時間及低操作電壓。裝置採用內電極配置，搭配中央控制電極並在電極之間旋塗上高電阻值材料，可以有效的使電能鎖在液晶層裡。同時，高電阻質材料也能提供在控制電極間平緩梯度的電場分布。和傳統液晶透鏡相比，此梯度控制液晶透鏡可將操作電壓從數十伏特降低至 5 伏特，配合過驅動方法，可將聚焦反應時間從三十秒降低至零點二秒。此種梯度控制液晶透鏡具有電力控制及可達成的光學變焦特性，不需機械操作，體積小，且耗電低聚焦反應時間短。十分適合結合至手機鏡頭模組中。

Gradient Driven Liquid Crystal Lens Exhibiting Ultra-Fast Focusing by Low Operating Voltage

Student: Yu-Min Lin **Advisor: Dr. Han-Ping D. Shieh**
Dr. Yi-Pai Haung

Abstract

Cell phone combined with camera function is the main trend in recent years. Most camera phones in present day utilize digital zoom function to zoom in. However, the image quality using digital zoom function is worse than using optical zoom function. Conventional optical zoom function is achieved by mechanical moving lens in a zoom lens system. Zoom lens require some volume to contain lots of lens components and have mechanical damage issue in long-term use. Applying the conventional zoom lens in the camera phone is a great challenge.

In this study, a tunable-focus liquid crystal lens exhibiting ultra-fast focusing and low operating voltage was proposed. The inside electrode configuration with a central controlling electrode is combined with a high resistance layer to conserve electric power efficiently. Moreover, the smooth gradient electric field distribution is maintained by the high resistance layer. Compared with conventional liquid crystal lens, this gradient driven liquid crystal lens (GD-LC lens) decreased the operating voltage from twenty more voltage to 5 voltages. And with using Over-Drive method, GD-LC lens decreased focusing response time from thirty seconds to 0.2 second. This GD-LC lens has unique characteristic such as electric tunable focus, no mechanical

moving part, small volume, low operating voltage and short response time which is suitable for camera phones application.

誌謝

第一件很感謝的是：很開心兩年的時間能在 LC 組裡面認真，很感謝俊賢、凌嶢的指導及討論，也很感謝 LF2、博元、欣怡的陪伴。唯有集合大家的努力不懈且集思廣益，才能有此篇論文的成果。

第二件很感謝的是：很開心在這個實驗室裡有許多好夥伴一起打鬧(就不一一列名了，你知道我心裡有你的，嘿嘿)，感謝有你們，讓我的生活更有趣更精彩，也在我低潮難過的時候幫我打氣，我會很懷念大家一起搭小紅巴吃中餐、一起運動打球的美好時光。

第三件很感謝的是：謝謝黃老師以及謝老師兩年來細心且耐心的指導，並提供良好的環境支持我。

第四件很感謝的是：謝謝我家人以及女友的支持，你們總是給我很大的力量繼續向前，希望未來的每一天都能像現在一樣，有一點開心、有一點煩惱，總是不無聊。

Table of Contents

Figure Captions

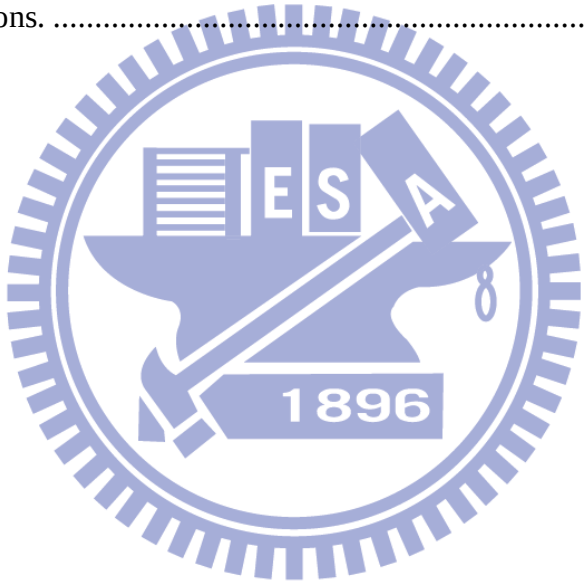

List of Tables

Chapter 1

Introduction

1.1 Zoom lens

Lenses are key elements of optical systems. Most conventional lenses, which have a fixed focal length, are made of glass, polymer, or other transparent solid materials. To tune the focal length continuously, a zoom lens, which is a mechanical assembly of lens elements with the ability to vary its focal length, has been developed. [1]

There are many possible designs for zoom lenses, the most complex ones having upwards of thirty individual lens elements and multiple moving parts. A simple scheme for a zoom lens divides the assembly into two parts: First is a focusing lens which is a fixed-focal-length photographic lens, preceded by a focal zoom system. Second is the focal zoom system which is an arrangement of fixed and movable lens elements that does not focus the light, but alters the overall magnification of the lens system, as shown in Fig. 1- 1 [2]. Obviously, numbers of lens components makes the zoom lens bulky and heavy. Many applications would benefit from a simpler, tunable-focus lens.

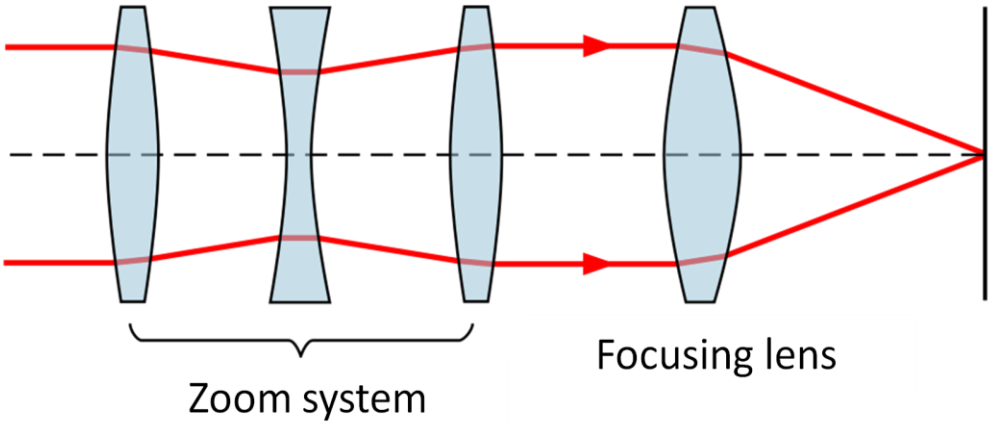

Fig. 1- 1 Schematic of simple zoom lens

In fact, a simple tunable-focus lens already exists in nature. For example, the human eye is a singlet lens system with a tremendously wide tunable focus range. By adjusting the muscles in the eye, the lens can be conformed to different shape to tune the focal length, as shown in Fig. 1- 2.

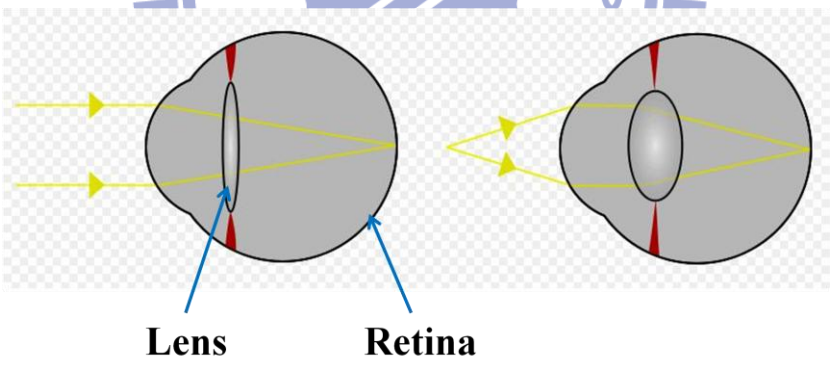

Fig. 1- 2 Schematic of the focusing mechanism of the human eye

To mimic the human eye's focusing system, some practical material approaches, such as liquid, microfluidics, and liquid crystal (LC), have been developed. By generating and controlling the optical path difference between the center and the edge of the lens, the focal length can be tuned through changing either shape or refractive index. These three kinds tunable-focal lens will be introduced in following sections.

1.2.1 Liquid lenses and microfluidic lenses

Liquid lenses and microfluidic lenses are examples of using shape changing to generate an optical path difference. According to the operation mechanism, liquid lenses and microfluidic lenses can be classified into two types.

The first type of liquid lenses and microfluidic lenses is based on the electrowetting phenomenon. The liquid lens uses two isodensity liquids, one is an insulator while the other is a conductor. The voltage applied to the substrate modifies the contact angle of the liquid drop. The variation of voltage leads to the liquid-liquid curvature interface changing, which in turn leads to lens focal length changing, as shown in Fig. 1- 3 [3].

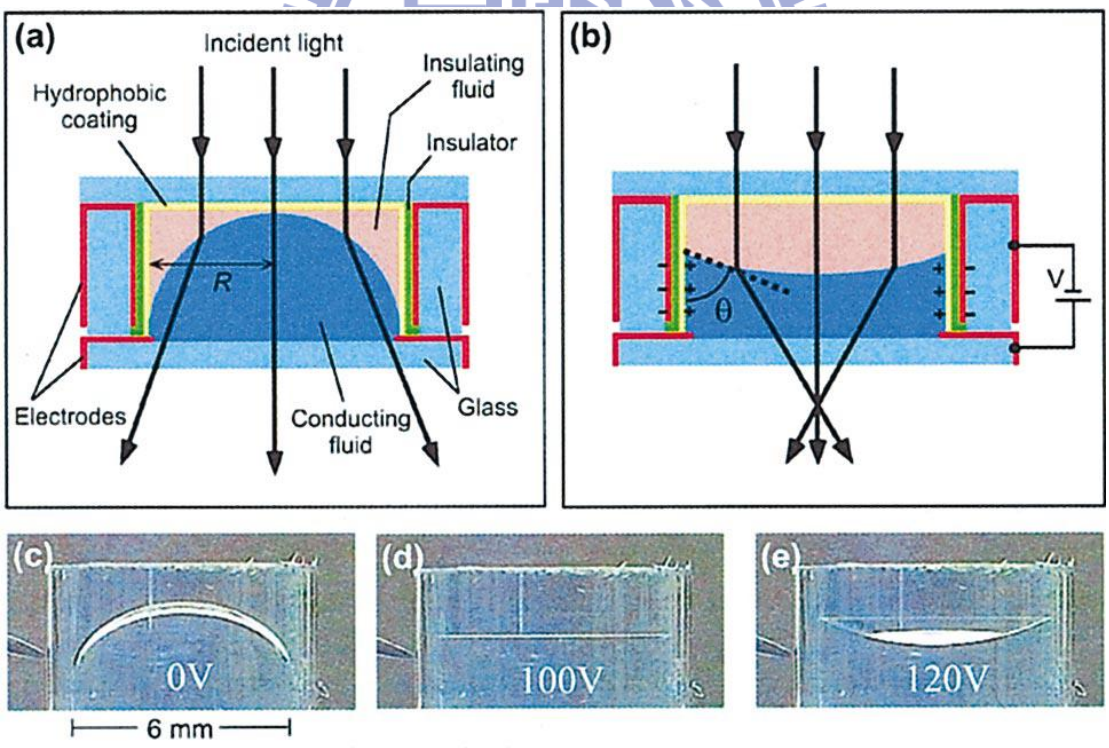

Fig. 1- 3 Schematic of eletrowetting type tunable-focal lens

The second type of liquid lenses and microfluidic lenses is based on the liquid pressure phenomenon. Through expanding or shrinking the liquid in a fixed volume

chamber, the liquid is conformed to the lens shape, as shown in Fig. 1- 4. The focal length is tuned by changing the curvature of the liquid shape. For example, in Fig. 1- 4, by applying a inward pressure to the outer membrane, the liquid redistributes and swells the inner membrane outward which forms a plano-convex lens [4].

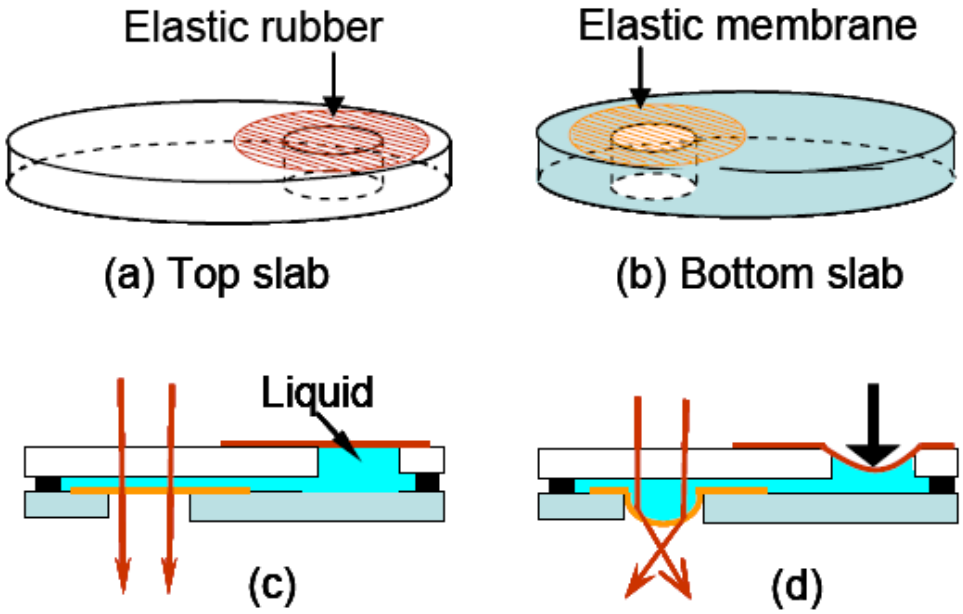

Fig. 1- 4 Structure of a liquid pressure type tunable-focal lens: (a) top slab, (b) bottom slab, and side view of the lens cell in (c) non-focusing state and (d) focusing state

1.2.2 Liquid crystal lenses

Liquid crystal lenses are examples of using refractive index changing to generate optical path difference. To make a LC lens, a gradient refractive index profile is necessary. Generally, the LC lens can be classified into: inhomogeneous LC alignment and homogeneous LC alignment types, as shown in Fig. 1- 5. The inhomogeneous LC alignment type has a serious issue, resulting in scattered light

because the LC molecular director suffers a nonuniform initial anchoring force [5][6]. Therefore, only the homogeneous LC alignment type is introduced in the following paragraphs.

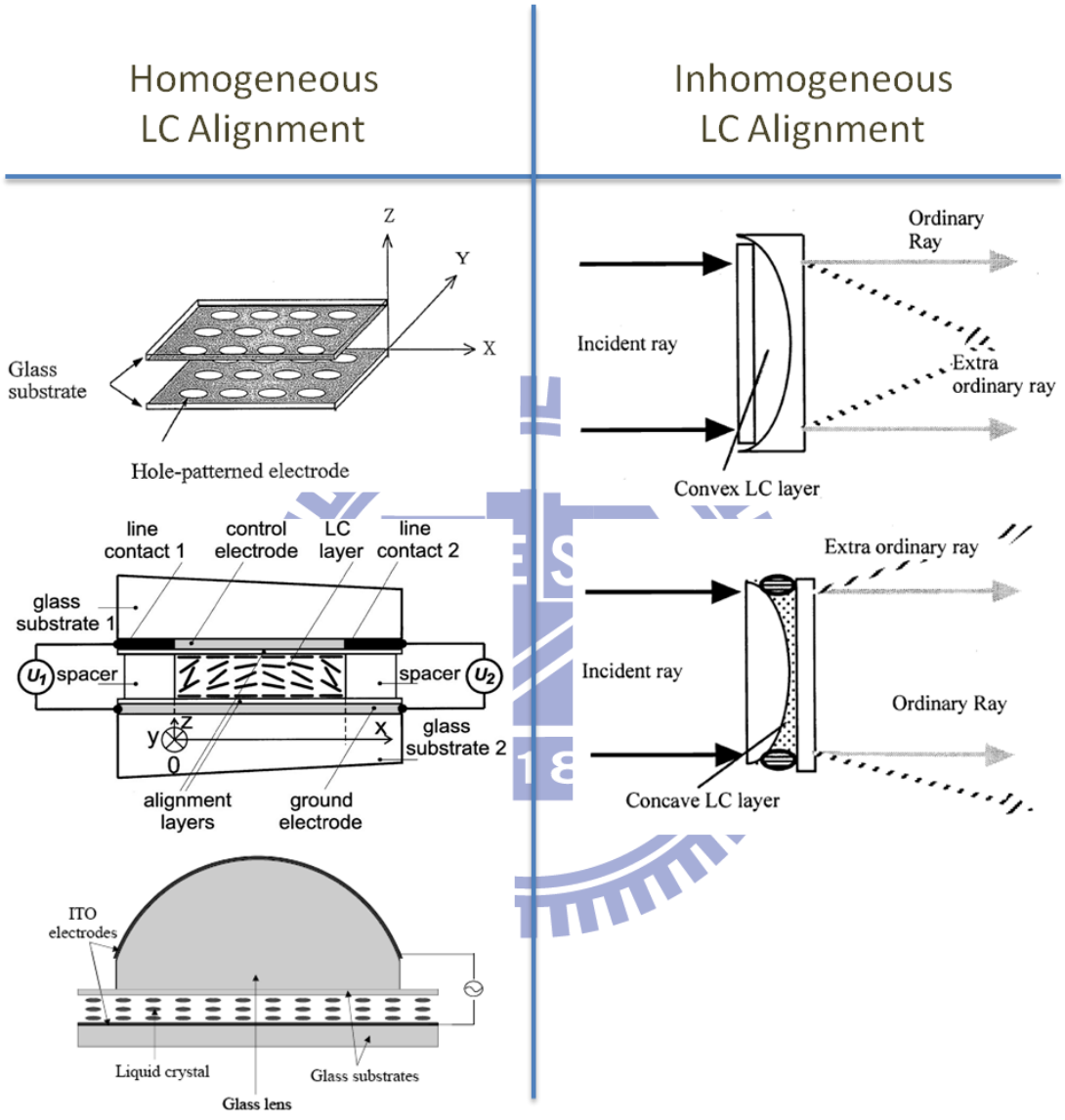

Fig. 1- 5 Different types of LC lenses

To generate the desired gradient refractive index profile in the homogeneous LC alignment, spatially varying electric field is necessary. Three methods for generating the gradient refractive index profile in the homogeneous LC alignment are considered here.

I. Patterned electrode type

The first approach is patterning the electrode to generate the smooth gradient electric field distribution. A continuous change of the focal length can be obtained by varying the applied voltage. The geometry chosen here is the most simple. Only one electrode being patterned is suggested. The electrode pattern whose form is not limited to circles is generally made by lithography. A schematic of cylindrical type LC lens is shown in Fig. 1- 6 [7].

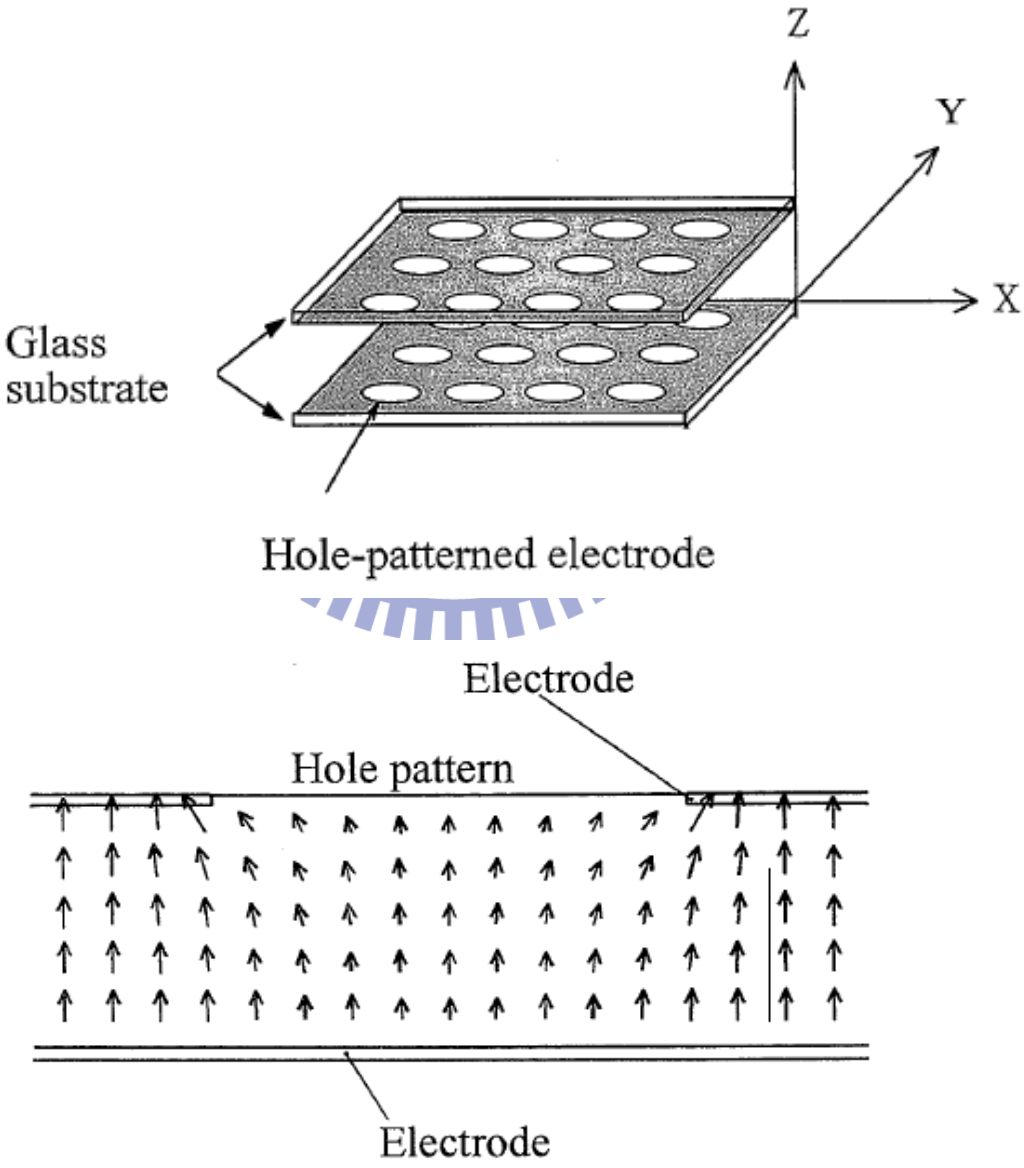

Fig. 1- 6 The schematic of cylindrical electrode patterned LC lens

II. Modal control type

The second approach is modal control. The key element of the modal lens is the control electrode, which should have high sheet resistivity (5 to 9 MΩ/M) across the aperture, as shown in Fig. 1- 7. The basic idea is to vary the electric field along the diameter of the lens. The electric field differs at various positions leading to different deformation strengths of the LC director. Modal control LC lens are simple to make and produce a smooth change in deviation angles or focal lengths by controlling the amplitude and frequency of the operating voltage. The major advantages of this approach are fast response and good image quality. However, such modal control LC lenses posses an aperture whose diameter is several millimeters. The numerical aperture (N.A.) is less than 0.005 which is insufficient [8].

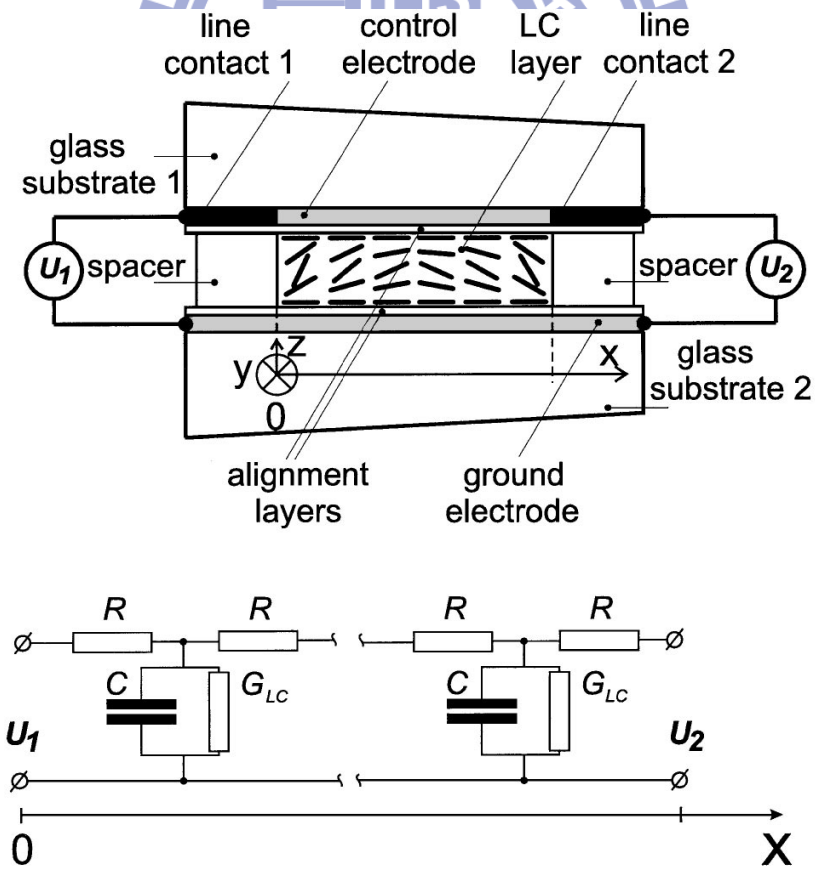

Fig. 1- 7 The schematic of modal control LC lens and its simplified equivalent circuit.

III. Flat spherical electrode type

The third approach, called flat spherical LC lens, uses an imbedded spherical electrode. The electric field from the spherical and planar electrodes induces a gradient refractive index distribution, as shown in Fig. 1- 8. The electric field strength redirects the LC and then changes the refractive index profile. This flat spherical LC lens provides a simple electrode design. Both convex and concave lens can be realized by reversing the shape of the spherical electrode. However, this LC lens suffers from slow response time [1][9][10].

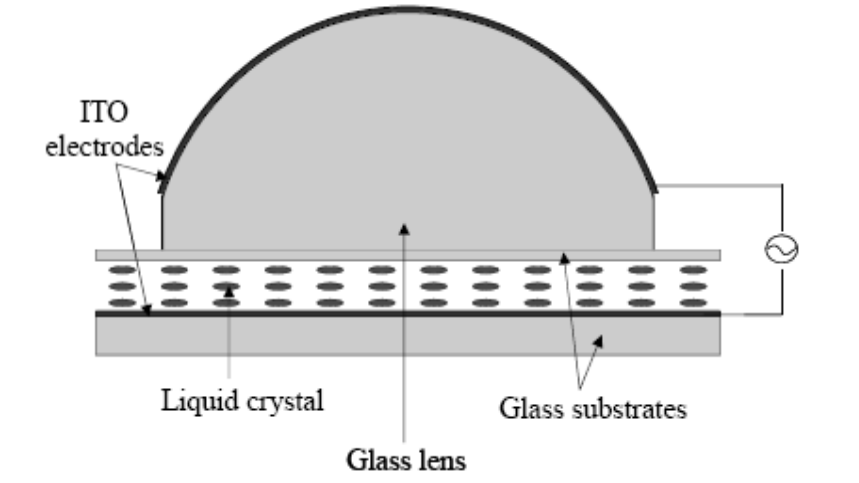

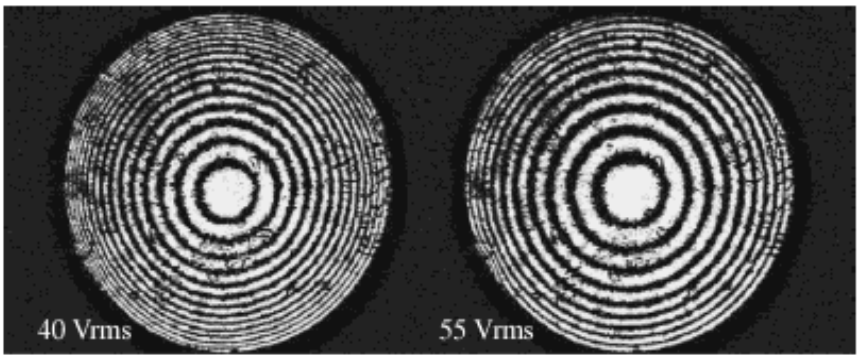

(a) (b)

Fig. 2. Interference fringes at $V = 40$ (a) and $55 V_{\text{rms}}$ (b).

Fig. 1- 8 The schematic of flat spherical LC lens.

1.3 Motivation and Objectives

A camera phone, as shown in Fig. 1- 9, is a mobile phone which is able to capture either image or video. Early in the 21st century the majority of cameras and of mobile phones in use have been camera phones. Camera phones are more portable than most digital cameras and allow people to stop images or films of an event being taken. More importantly, they offer faster connection with the internet so we can share the images and film around the world instantly [11].

Fig. 1- 9 Picture of camera phone

According to a report from InfoTrends entitled "Worldwide Camera Phone Forecast: 2007-2012", worldwide shipments of camera phones will jump from over 700 million units in 2007 to surpass 1.3 billion in 2012. Mobile video services are also expected to grow rapidly in the years to come. Detractors of mobile video have previously cited poor phone quality as one of the biggest reasons why these services have yet to take off. However, with the launch of more viewer-friendly phones, such as the iPhone, mobile video services are expected to quickly gain popularity. Worldwide revenues from mobile video will nearly triple to reach USD 18.2 billion by the end of

2013 [12][13].

Most camera phones are simpler than digital cameras. Their usual fixed focus lenses and smaller sensors limit their performance in poor lighting, and most have a long shutter lag. However, to zoom in on your subject when taking your picture is desirable. When using a digital zoom, the image quality decreases. With the increase of using camera phones, the auto-focusing (AF) requirements and optical zoom function have become critical. Thus, the AF and optical zoom function combined with camera phones will benefit users [14].

In fact, the current tunable-focal lens module is not suitable for camera phone application. Conventional zoom lens is heavy and bulky. To tune the focal length, the mechanical movement is necessary. Obviously, conventional zoom lens is not suitable for camera phone application. Nowadays, most camera phones use only the digital zoom function to simulate the real image which decreases the image quality. To overcome these issues, several approaches were reported. The LC lens method is the focus of this thesis (see 1.2.2).

The LC lens has unique properties such as electrically tunable focal length. Since there are no moving mechanical parts, the LC lens is smaller and lighter than conventional tunable glass lenses. The major technical challenge of LC lens is generating a gradient refractive index instantaneously after applying operating voltage [15]. However, long focusing time is a serious issue in the study of LC lenses. The LC cell gap is thick which yields high optical power requiring high operating voltage to shorten focusing time. The objective in this thesis is to reduce long response time and high operating voltage in LC lens.

Therefore, using the modal control concept, a fast focusing gradient driven LC (GD-LC) lens is proposed. The configuration of triple internal electrodes connected by

a high resistance layer efficiently conserved electrical energy inside the LC layer and initially generated a large potential difference between the center and border of the lens. To be practical applicable, the focusing time and the operating voltage need to be improved less 1second and 10 Volt respectively.

1.4 Organization of this thesis

This thesis is organized as follows: In chapter 2, some basic principles and theories in LC lens such as LC director calculation, effective focal length, response time, and modal control lens will be introduced. In chapter 3, the fabrication process and the experimental setup will be clearly presented. In chapter 4, the electrode configuration design of the GD-LC lens will be illustrated. In chapter 5, the experimental result of the GD-LC lens will be demonstrated and discussed. Finally, in chapter 6 the conclusions and future works will be given.

Chapter 2

Basic principles and theories in LC lens

2.1 LC Material

Liquid crystal (LC) is a state between liquid and solid crystal. For example, LC may flow like a liquid, but may be oriented like a crystal. According to optical properties, the LC can be classified into five types: nematic phase, smetic phase, chiral phase, blue phase, and discotic phase [16]. The nematic LC is used in this thesis.

Nematic LCs, as shown in Fig. 2- 1, have fluidity similar to that of ordinary (isotropic) liquids but they can be easily aligned by an external magnetic and electric field. An aligned nematic LC has the optical properties of a uniaxial crystal making it extremely practical.

Fig. 2- 1 Nematic LC

2.2 LC Director Calculation

In a uniform state, LC has a structure characterized by position independent order parameters. When the LC molecules are limited by the walls of a container or external fields (magnetic, electric, and so on), the LC becomes deformed. Since deformations cost energy, they are accompanied by restoring forces that oppose the deformations. To describe this phenomenon, it is convenient to regard the LC as a continuum with a set of elastic constants. Thus, energy density can be described in following form [17]:

$$\mathbf{f(r) = f_0 + f_d(r) + f_e(r)} \qquad \textbf{Eq. 2- 1}$$

Where r is the LC molecular position, f_0 represents the free energy density of a uniform state, $f_d(r)$ represents the elastic free energy density, and $f_e(r)$ represents the energy density contributed to external fields. Generally, $f_e(r)$ is opposite in polarity to $f_d(r)$. In nematic LC, molecules can be regarded as a system consisting of rotationally symmetric ellipsoids, as shown in Fig. 2- 2. The orientation of nematic LC can be described using unit vector **n**, so called the "director". There is a standard expression, the Frank expression, for elastic free energy density:

$$\mathbf{f_d} = \frac{\mathbf{1}}{\mathbf{2}}\mathcal{K}_{\mathbf{11}}(\nabla \cdot \mathbf{n})^{\mathbf{2}} + \frac{\mathbf{1}}{\mathbf{2}}\mathcal{K}_{\mathbf{22}}\big(\mathbf{n}(\nabla \times \mathbf{n})\big)^{\mathbf{2}} + \frac{\mathbf{1}}{\mathbf{2}}\mathcal{K}_{\mathbf{33}}\big(\mathbf{n} \times (\nabla \times \mathbf{n})\big)^{\mathbf{2}} \qquad \textbf{Eq. 2- 2}$$

Where $\mathcal{K}$ represents elastic constant. $\mathcal{K}_{11}(\nabla \cdot n)^2$ denotes splay state. $\mathcal{K}_{22}\big(n(\nabla \times n)\big)^2$ denotes twist state, and $\mathcal{K}_{33}\big(n \times (\nabla \times n)\big)^2$ denotes bend state. Three possible deformations in nematic LC are clearly illustrated in Eq.2-2 and shown in Fig. 2- 3.

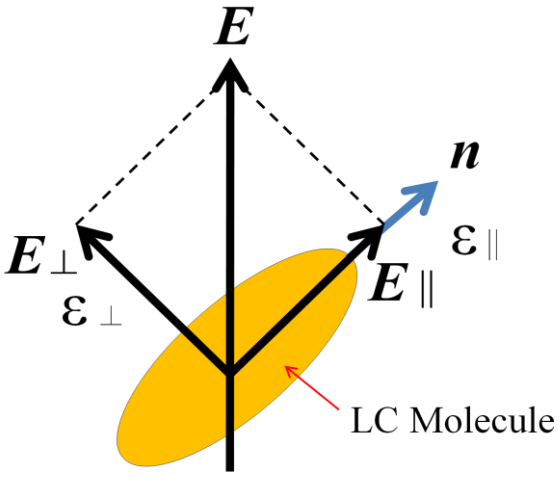

Fig. 2- 2 The schematic showing nematic LC

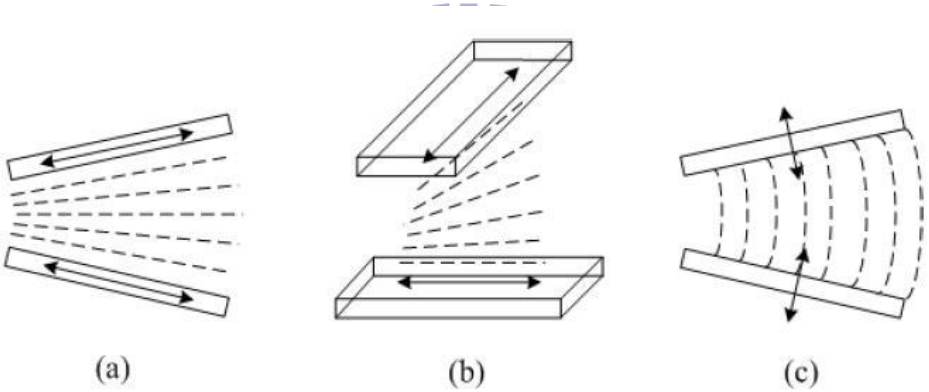

Fig. 2- 3 Three possible deformations in nematic LC layer

The LC dielectric anisotropy is defined as $\Delta\varepsilon = \varepsilon_{\parallel} - \varepsilon_{\perp}$. To calculate the director profile in the LC layer, both elastic deformations and the external electric field have to be considered. The external electric field can be represented as follows:

$$\mathbf{f_e} = \frac{\mathbf{1}}{\mathbf{2}}\mathbf{E}\cdot\mathbf{D} \quad \textbf{with} \quad \mathbf{D} = \boldsymbol{\varepsilon}\boldsymbol{\varepsilon_0}\mathbf{E} \qquad \textbf{Eq. 2- 3}$$

Where $\boldsymbol{\varepsilon}$ is the dielectric tensor of LC, **E** is the electric field, and **D** is electric displacement. The dielectric tensor changes when the LC is reoriented. The positive type nematic LC ($\Delta\varepsilon > 0$) will follow the applied electric field direction to remain electric free energy and free energy in the lowest state, and vice versa.

2.3 Anchoring Effect

In most LC devices, the LC layer is sandwiched between two substrates coated with an alignment layer. LC alignment, which is achieved by the anchoring effect, affects the equilibrium state and director profile in the LC layer. By varying the alignment directions of the top and bottom substrates, the LC can be aligned into different LC configurations, as shown in Fig. 2- 44. The tilted planar LC configuration is adopted in this thesis.

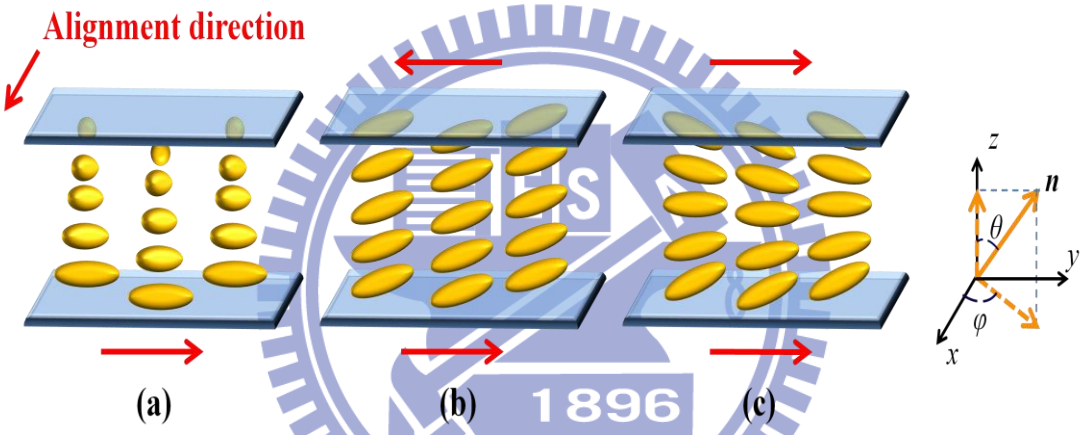

Fig. 2- 4 Three alignment arrangements of top and bottom substrates in (a) twist-nematic, (b) tilted planar, and (c) pi-cell

Generally, the polyimide is used here as alignment material because of its low cost, high stability, and easy fabrication.

The anchoring free energy density can be expressed by the Rapini-Papoular approach as follows [18]:

$$f_s = f_\theta + f_\varphi$$

$$f_\theta = \frac{1}{2} W_\theta sin^2(\theta - \theta_0)$$

$$f_\varphi = \frac{1}{2} W_\varphi sin^2(\varphi - \varphi_0) \qquad \textbf{Eq. 2- 4}$$

where θ and φ denote polar and azimuthal angles, f_s denotes the total free energy resulting from the anchoring effect, f_θ denotes the free energy component in terms of the polar angle, f_φ denotes the free energy component in terms of the azimuthal angle. W_θ and W_φ are the constants whose physical meanings are the interactions between the substrates and the LC director. θ_o and φ_o are the equilibrium angles in the polar and azimuthal dimensions respectively. By considering the anchoring effect, Eq.2-1 can be modified as:

$$\mathbf{f(r) = f_0 + f_d(r) + f_e(r) + f_s(r)} \qquad \textbf{Eq. 2- 5}$$

2.4 LC Lens

Liquid crystal materials have been widely used for display technology and other electro-optic devices due to their unique physical properties. By applying an inhomogeneous electric field, a gradient index refraction distribution can be generated in a homogeneous LC layer. Therefore, the LC device can achieve lens effect by controlling the optical path difference between the center and the edge of the LC device [19][20]. For example, Fig. 2- 5 shows how convex type LC lens work.

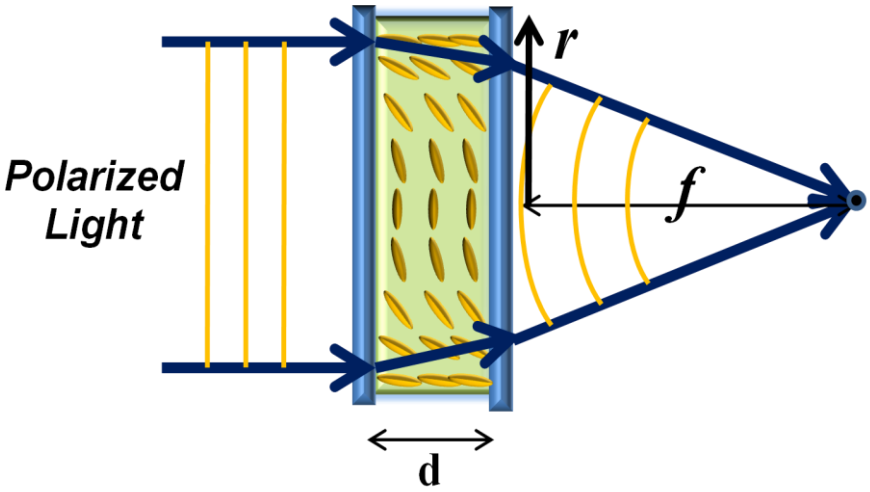

Fig. 2- 5 The schematic of LC lens

To design a high quality LC lens, effective focal length and response time have to be considered. The following sections will introduce these two factors.

2.4.1 Effective focal length

Nematic LC material has a birefringence property including ordinary refractive index and extraordinary refractive index. When an electric field is applied to the LC cell, the LC is reoriented and its tilt angle is changed. The director is rotated and an effective refractive index has to be considered which is dependent on the degree of the LC's tilt angle. The effective refractive index can be calculated using the following equation [21]:

$$n_{eff}(\theta) = \frac{n_o n_e}{\sqrt{n_e^2 sin^2\theta + n_o^2 cos^2\theta}} \qquad \textbf{Eq. 2- 6}$$

where the θ denotes the angle between the polarization of incident light and LC optical axis, and the n_e and n_o denote the refractive index for the ordinary light beam and the extraordinary light beam.

To derive the effective focal length in LC lens, incident polarized light is

assumed to be planar wavefront. Since every point in the same wavefront should pass the same optical path, this incident planar wavefront will bend into a spherical wavefront. For example, Fig. 2- 6 shows how a convex type LC lens focuses light.

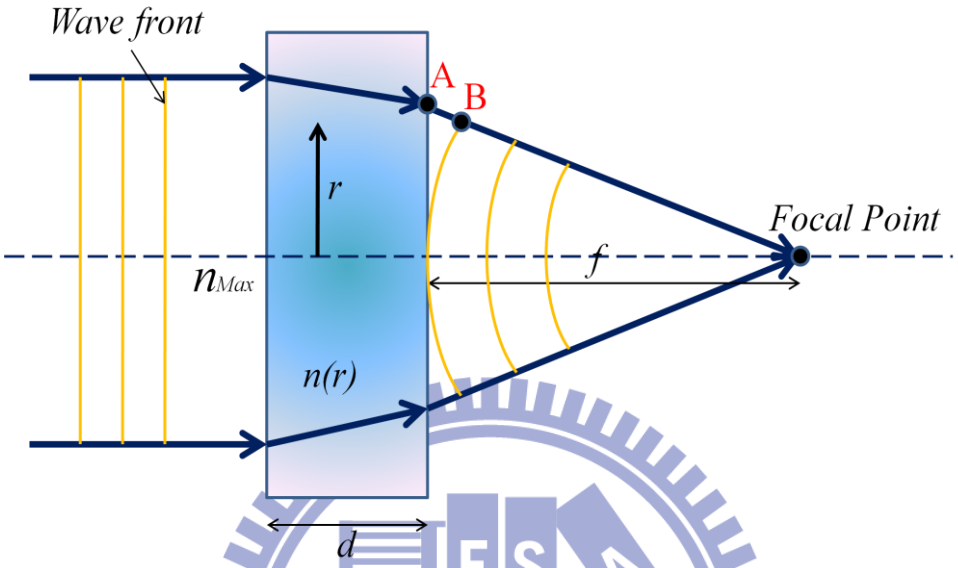

Fig. 2- 6 The schematic showing focusing mechanism of convex type LC lens

In the example in Fig. 2- 6, the optical path between the center position and edge position can be expressed as follows:

$$\boldsymbol{n(r)d + AB = n_{Max}d}$$

$$\boldsymbol{\Rightarrow\ AB = [n_{Max} - n(r)]d} \qquad \textbf{Eq. 2- 7}$$

Furthermore, the distance AB can be expressed as:

$$\boldsymbol{AB = AF - f} \qquad \textbf{Eq. 2- 8}$$

$$\textbf{where } \boldsymbol{AF = \sqrt{r^2 + f^2}}$$

Combining Eq.2-7 and Eq.2-8, the optical path can be expressed as:

$$[n_{Max} - n(r)]d + f = \sqrt{r^2 + f^2}$$

$$\Rightarrow\ n_{Max} - n(r) = \frac{\sqrt{r^2+f^2}-f}{d} \qquad \textbf{Eq. 2- 9}$$

Because the effective focal length, f, is much higher than the lens radius value, r, the Fresnel' approximation is used as follows [22]:

$$\sqrt{r^2 + f^2} \approx f\left[1 + \frac{1}{2}\left(\frac{r}{f}\right)^2\right]$$

$$\Rightarrow\ n(r) = n_{Max} - \frac{f\left[1+\frac{1}{2}\left(\frac{r}{f}\right)^2\right]-f}{d} = n_{Max} - \frac{r^2}{2fd}$$

$$\Rightarrow\ f = \frac{r^2}{2d[n_{Max}-n(r)]} = \frac{r^2}{2d\cdot\Delta n} \qquad \textbf{Eq. 2- 10}$$

Through transposing of Eq.2-10, another representation of Δn can be expressed as shown in Eq.2-11.

$$\Delta n = \frac{r^2}{2d_{LC}f} = \kappa r^2 \qquad \textbf{Eq. 2- 11}$$

Ideally, every part of the lens should fit the same focal point or aberrations will be observed. According to Eq.2-11, Δn shall be a parabolic function of r^2, as shown in Fig. 2- 7.

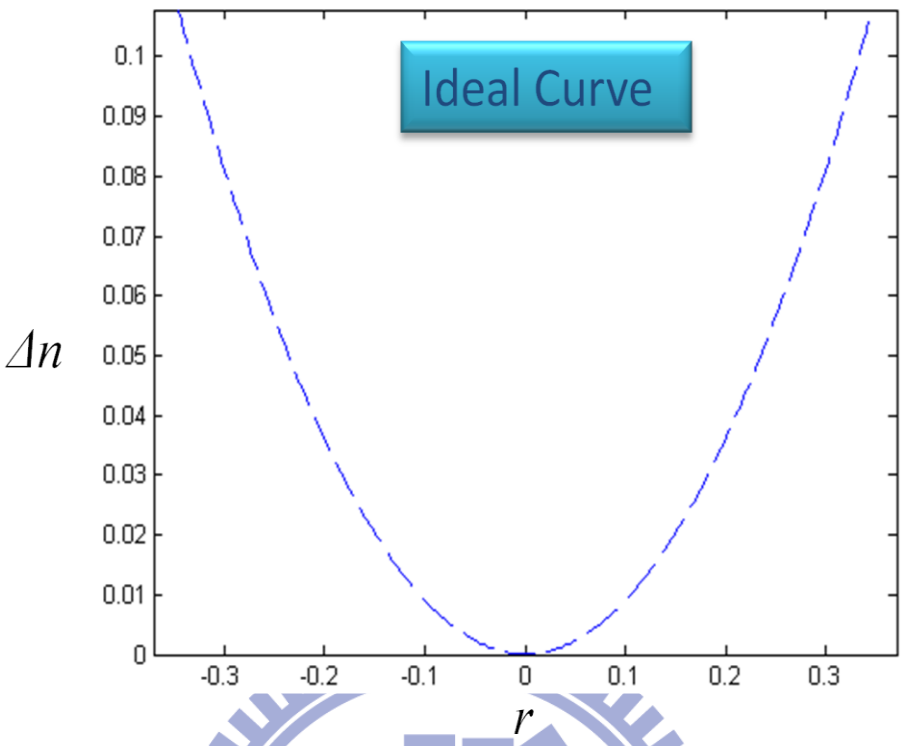

Fig. 2- 7 The ideal parabolic curve function of Δn and radius of lens aperture

2.4.2 Response time

Though there is no standard method to accurately measure the response time of the LC lens, the response time characteristic can still be derived by using the Erickson-Leslie equation. In a homogeneous LC layer, when twist deformation, backflow effect, and inertia effect are ignored, the dynamic response time can be described as follows [23]:

$$(K_{11}cos^2\theta + K_{33}sin^2\theta)\frac{\partial^2\theta}{\partial Z^2}$$

$$+(K_{33} - K_{11})sin\theta cos\theta\left(\frac{\partial\theta}{\partial Z}\right)^2$$

$$+\varepsilon_0\Delta\epsilon E^2 sin\theta cos\theta = \gamma_1\frac{\partial\theta}{\partial t} \qquad \text{Eq. 2- 12}$$

where E denotes the applied voltage, and γ_1 denotes the rotational viscosity.

In small angle approximation, the rise and decay response times of the LC cell can be described as follows:

$$\tau_{rise} = \frac{\gamma_1 d^2 / K\pi^2}{(V/V_{th})^2 - 1} \quad \text{Eq. 2- 13}$$

$$\tau_{decay} = \frac{\gamma_1 d^2 / K\pi^2}{\left|(V_b/V_{th})^2 - 1\right|} \quad \text{Eq. 2- 14}$$

where d denotes the LC cell gap, K denotes the elastic constant, V_{th} denotes the threshold voltage, V_b denotes the bias voltage, and V denotes the applied voltage. Obviously, after setting the LC material parameters, the rise time and decay time are proportional to LC layer thickness and the reciprocal of external electric field energy.

2.5 Modal Control LC Lens

A modal control LC lens is shown in Fig. 1- 7. An LC layer is sandwiched between two glass substrates on which plane electrodes are deposited. The surface resistance of the control electrode is much higher than the resistance of the ground electrode. The control voltage is applied to contacts located at the control electrode periphery. The initial uniform orientation of the LC layer is determined by the alignment layer. The thickness of the LC layer is set by the thickness of the spacers separating the glass substrates.

The physical mechanism of the formation of a controlled phase retardation profile is as follows. If a sinusoidal control voltage is applied to the contacts, the changes in the voltage at the center of the control electrode lag behind the changes in the voltage applied to the contact electrodes because of the resistive-capacitative nature of the system. An increase in the frequency of the applied voltage increases the

delay and reduces the rms value of the voltage at the center of the aperture. This phenomenon is enhanced also by leakage currents across the LC layer. Under steady state conditions, the distribution of the rms voltage in the LC layer falls from the edge of the control electrode to its center, as if a parabolic curve. This is important from a practical point of view because when the operating voltage range corresponds to the linear part of the voltage-phase characteristic, the resultant adaptive LC lens may be close to ideal [24].

The equivalent circuit of modal control LC lens, shown in Fig. 1- 7, is similar to a transmission line in the case of dielectric losses and not of conduction currents. The voltage profile across the device is described by the following partial differential equation: [25]

$$-\frac{\partial U}{\partial x} = (R + j\omega L)I(x)$$

$$-\frac{\partial I}{\partial x} = (G + j\omega C)U(x) \quad \text{where L=0}$$

Then $$\frac{\partial^2 U}{\partial x^2} = j\omega RCU + RGU \qquad \textbf{Eq. 2- 15}$$

where U, is the voltage, R is the sheet resistance of the control electrode, and C and G are the capacitance and conductance per unit length of the LC layer.

According to Eq .2-15, if the control voltage is sinusoidal, the amplitude of the voltage is as follows:

$$\nabla_s^2 U = \chi^2 U \qquad \textbf{Eq. 2- 16}$$

$$\textbf{Where } \chi^2 = \rho_s(g - j\omega c)$$

Where ρ_s, **g,** and **c** represent the sheet resistance of the control electrode, the conductivity of the LC layer per unit are, and the capacitance of the control electrode

per unit area. The voltage distribution is governed by χ. The distribution of **U(x,y)** differs from χr (r is the radius of lens aperture). The LC impedance is defined as following:

$$Z_s = (g - j\omega c)^{-1}$$

$$\text{Then } (\chi r)^2 = \rho_s r^2 / Z_s \qquad \text{Eq. 2- 17}$$

Where χr represents the ratio of the resistance of the high resistance electrode to the impedance of the LC layer. The frequency dependence of χ allows the voltage distribution to be controlled by altering the control voltage frequency. To investigate the voltage distribution numerically in the modal control LC lens, the approximate solution is obtained by setting $Z_s = \text{const}$.

I. Cylindrical type

The voltage distribution in this geometry becomes:

$$\frac{d^2U}{dx^2} = \chi^2 U \qquad \text{Eq. 2- 18}$$

The boundary condition is set as:

$$U(-r) = U_{01} \sin \omega t, \; U(r) = U_{02} \sin(\omega t + \varphi) \qquad \text{Eq. 2- 19}$$

When $U_{01} = U_{02} = U_0$, and $\varphi = 0$, the voltage distribution can be expressed according to Eq.2-18 and Eq.2-19:

$$U = U_0 \frac{\cosh(\chi x)}{\cosh(\chi r)} \qquad \text{Eq. 2- 20}$$

Fig. 2- 8 shows the calculated value of the voltages at different frequency between contacts. Apparently, operating frequency alters the voltage distribution. The conductance and capacitance of LC, which both are dependent of amplitude and frequency, can be regarded as constants because the calculated results whether or not to consider the conductance and capacitance as variables are almost the same.

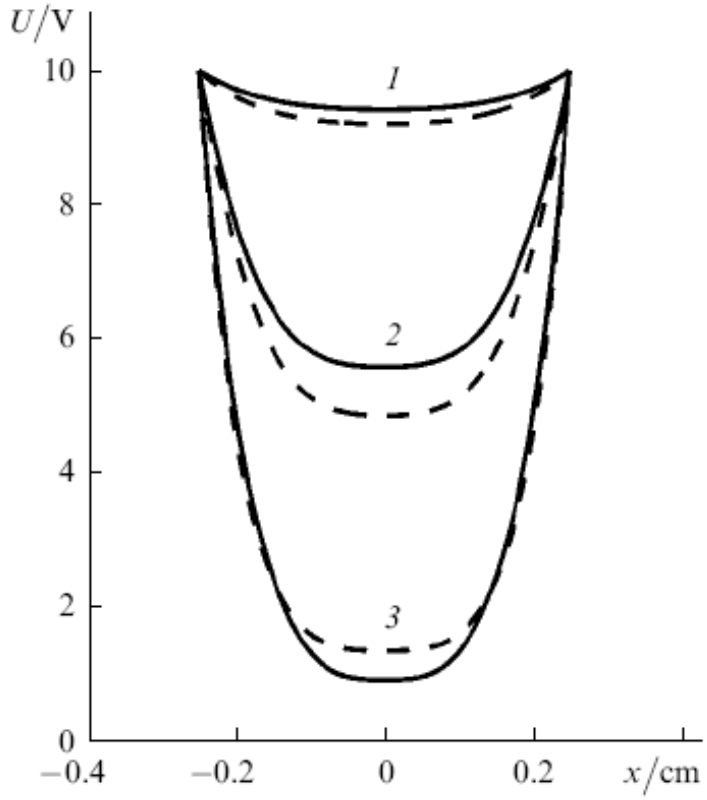

Fig. 2- 8 Distributions of the voltages along a selected coordinate, calculated at frequencies 2 kHz (1), 10 kHz (2), and 45 kHz (3). The voltage applied to the contacts is assumed to be 10 V, 2R= 5 mm; the dashed curves are the result of a numerical calculation which takes account of the voltage dependences of g and c

If $\boldsymbol{\chi r}$ is large, the voltage falls exponentially from a contact to the center of the aperture and differs considerably from zero only in a narrow region whose width is of the order of $\boldsymbol{\chi^{-1}}$. This region is not suitable for forming a modal control LC lens.

II. Spherical type

The voltage distribution in this geometry becomes:

$$\frac{d^2U}{dr^2} + \frac{1}{r}\frac{dU}{dr} - \chi^2 U = 0 \qquad \text{Eq. 2- 21}$$

When the boundary condition is set as:

$$U(r = R) = U_0 \qquad \text{Eq. 2- 22}$$

The solution is in the following form:

$$U = U_0 \frac{J_0(ir\chi)}{J_0(iR\chi)} \qquad \text{Eq. 2- 23}$$

2.6 Summary

The basic principles and theories of LC material were introduced in this chapter. To design an LC lens, the mechanism, effective focal length, and response time were presented. In chapter 4, these properties will be used to optimize the LC lens' specification. Moreover, because the GD-LC lens is designed based on modal control LC lens structure, the voltage distribution characteristic, which is affected by both amplitude and frequency, was discussed.

Chapter 3

Fabrication process and experimental setup

In the first part of this chapter, the fabrication process of LC lens will be reported step by step. The process includes cleaning glass substrates, lithography, coating thin film, and assembling sample.

In the second part of this chapter, the experimental setup to measure the focusing profile and the interference pattern will be illustrated. Moreover, the over-drive method which is adopted to reduce response time of the LC lens will also be introduced.

3.1 Fabrication process

The basic fabrication processes is as shown in Fig. 3- 1. First of all, the ITO glass substrates need to be cut into suitable size. Second, the ITO glass substrates are cleaned. This step is very important because any particles allow image defects exiting. Third is the lithography fabrication processes including spin coating, photomask generating, UV light exposing and wet etching. Fourth, some materials needs to be spin coated on the glass substrates. Finally, the glass substrates, spacer, LC materials will be assembled. After finishing assembling sample, the ITO pattern will be soldered with wires to accomplish the full fabrication process.

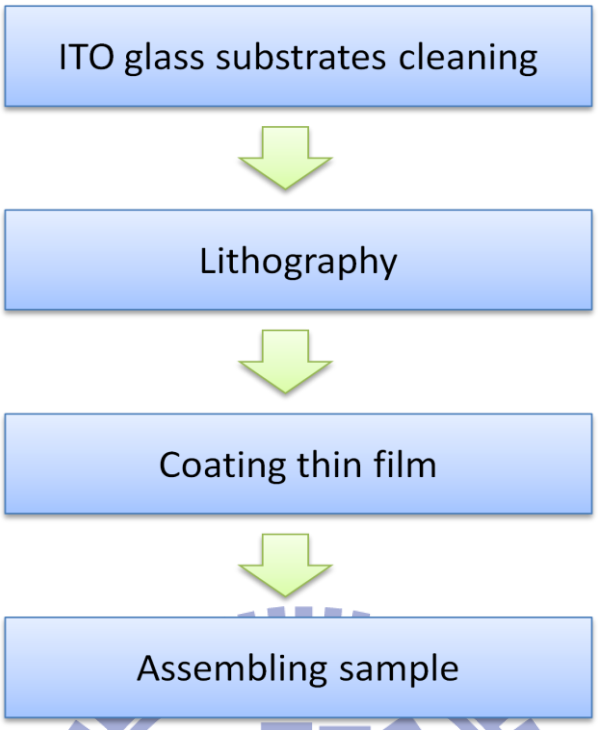

Fig. 3- 1 The flow chart of fabrication process

3.1.1 Cleaning glass substrates

Cleaning ITO glass substrates is very crucial for the following steps. The purpose of this step is to removes particles and chemical impurities from the surface without damaging or altering the substrate surface. The flow chart of this cleaning process is as shown in Fig. 3- 2. First of all, Acetone is used to clean the organic leftover on the substrates. Acetone can also be used to clean the photoresist. Second, these substrates need to be scrubbed by the hands with the detergent. Because the ITO and glass substrates are the hydrophilic material, the water distribution can distinguish the cleanliness. The sprayed water on the substrate uniformly distributed implies that the substrate is clean. Thirdly, the de-ionized (DI) water is used to clean the substrates. Finally, the heater is used to evaporate the left water.

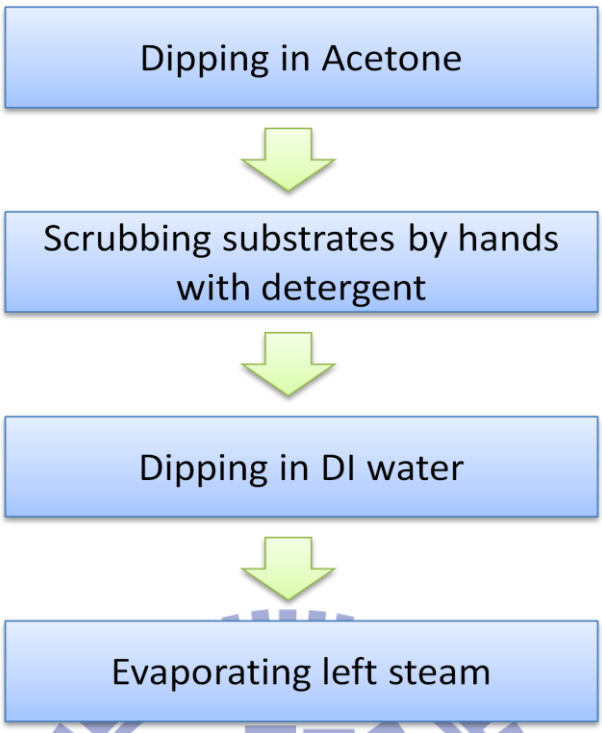

Fig. 3- 2 The flow chart of cleaning process

3.1.2 Lithography

Lithography technology is adopted to transfer specific patterns from the photomask onto a ITO glass substrate. The desired patterns were generated by the lithography processes, as shown in . First of all, the spin coater was used to generate the uniform and thin photoresist layer on the surface of the ultra clean glass substrate. A photoresist acts similarly to the sensitizer of a film in a camera since it could optically transfer the patterns of the layout from the photomask. Second, the UV light beam incidents the photomask which has our designed patterns and reacts with the chemical component of the photoresist. Third, the chemical reacted photoresist can be stripped off and remains the no chemical reacted parts. Therefore, our desired patterns are generated on the photoresist after the exposures photoresist is developed. Further, the left photoresist is like a protective layer to its cover ITO part. Therefore, HCl is used to etch the ITO layer which has no photoresist covered part. Finally, stripping the

left photoresist and our designed ITO pattern is generated.

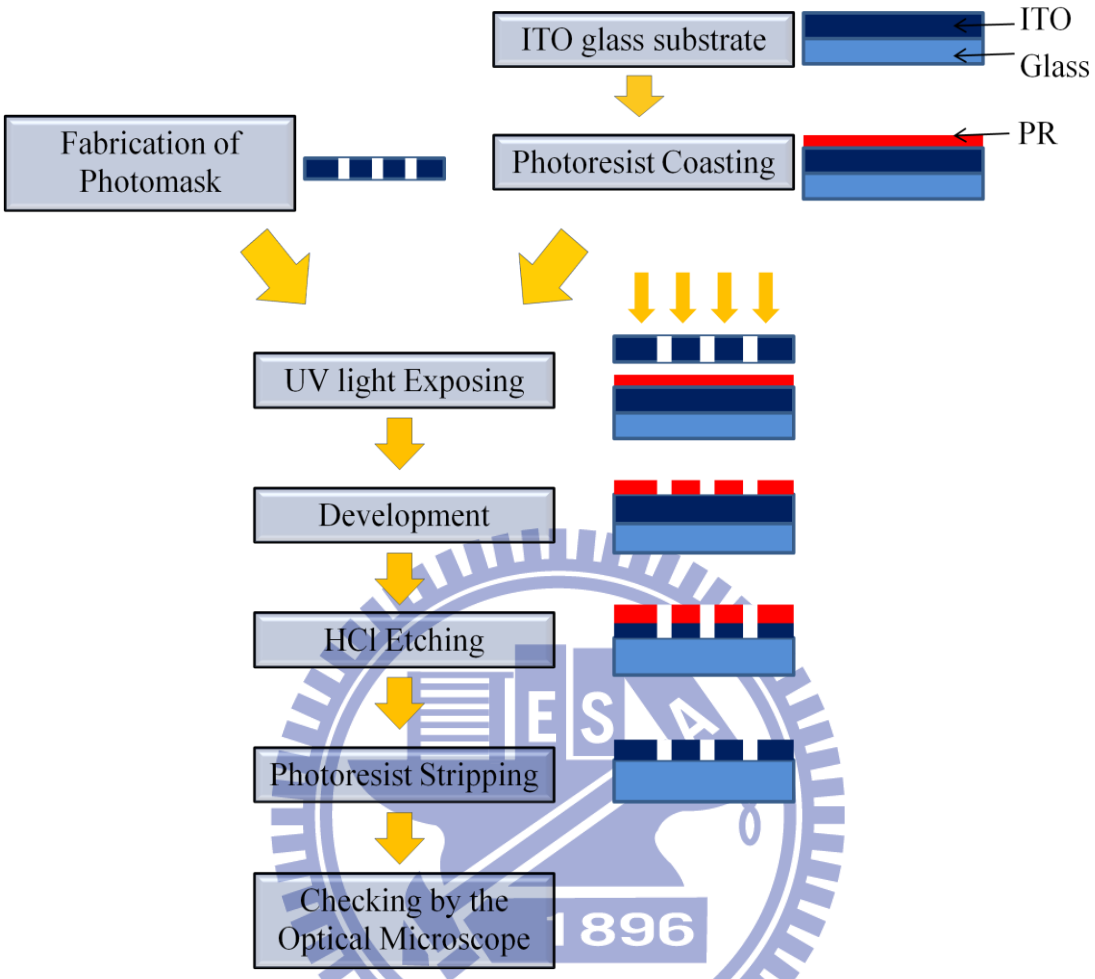

Fig. 3- 3 The flow chart of lithography process

3.1.3 Coating thin film

Spin coating is a procedure used to apply uniform thin films to flat substrates. In short, an excess amount of a solution is placed on the substrate, which is then rotated at high speed in order to spread the fluid by centrifugal force. A machine used for spin coating is called a spin coater, or simply spinner.

Rotation is continued while the fluid spins off the edges of the substrate, until the desired thickness of the film is achieved. The higher angular speed of spinning obtains the thinner the film. The thickness of the film depends on the concentration of the

solution and the solvent.

Three different materials have to be spin coated during the modal control LC lens fabrication process. First is the photoresist which is mentioned in lithography process (see 3.1.2 Lithography). Second is a high resistance material which is connected with ITO pattern and is used to achieve spatial varying electric field distribution. Third is polyimide (PI) which is commonly used as alignment layer in LC devices.

3.1.4 Assembling sample

This step is used to assemble the whole LC device, and the flow chart of the assembly process is as shown in Fig. 3- 4. After the substrates being prepared, the roller with woolen texture is used to rub on the PI coated substrate. Second, the spacers are pasted on the substrates to sustain the cell gap, and the top and bottom substrates are assembled which in anti-rubbing direction arrangement. Further, the glue is used to fix and seal one side of the LC cell. Fourth, the LC material is injected into the cell. Then, the glue is used to seal all the seams of the LC cell completely in order to prevent the LC material contact with the air. Finally, soldering the wires with the pattern on substrate, the LC lens is accomplished.

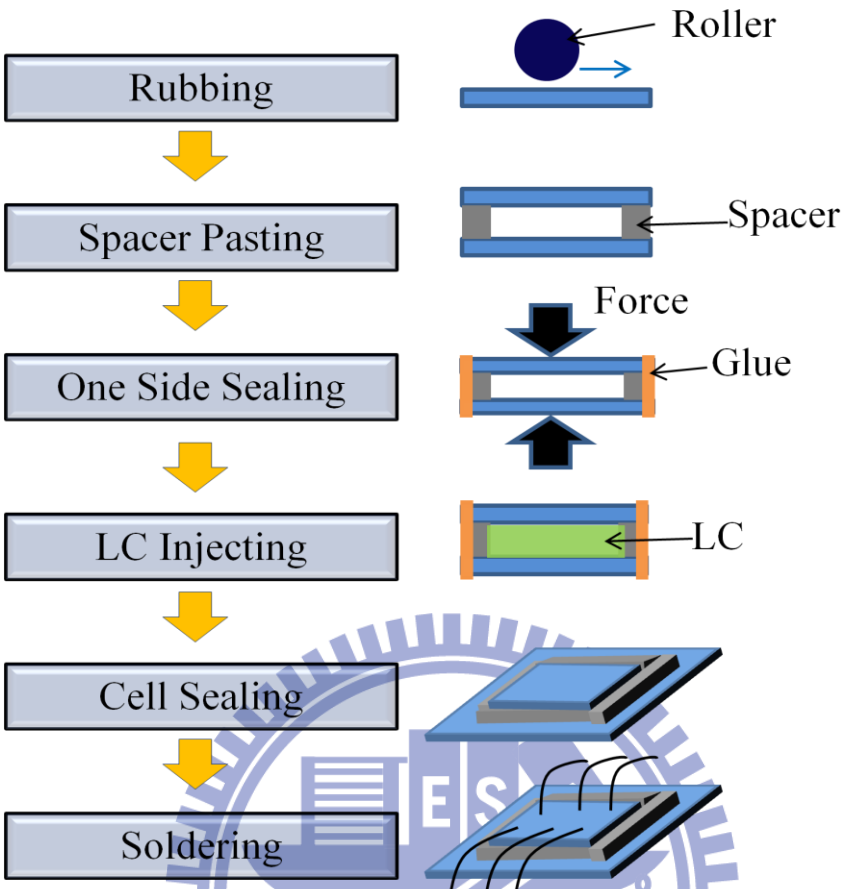

Fig. 3- 4 The flow chart of assembling sample

3.2 Experimental setup

After accomplishing the LC lens sample, the focusing profile and the interference pattern need to be measured. These two results judge whether the sample owns desired performance.

3.2.1 Measurement system

The measurement system is constructed with using following components: polarized He-Ne laser whose 632.8 nm wavelength, beam expander, pin hole, polarizer, LC lens sample, and GENTEC Beamage Series CCD sensor, as shown in Fig. 3- 5.

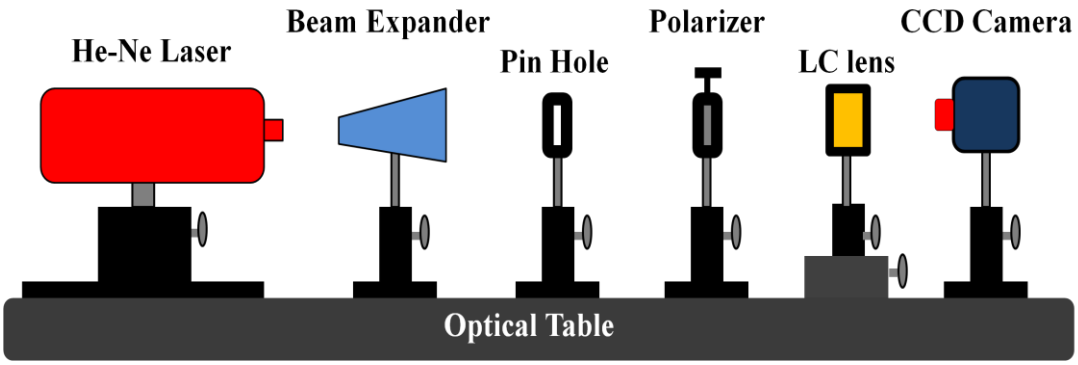

Fig. 3- 5 Schematic of measurement system

To investigate the focusing profile of LC Lens, the device is set up in front of GENTEC Beamage Series CCD sensor at a distance of corresponding focal length. The controlling electrodes are driven at 1 kHz. As the operating voltage was V=0, the incident light passes through the device directly without focusing, As Fig. 3- 6(a) shows. The top and bottom figures of Fig. 3- 6 indicate the top-view and cross-section of the measured beam profile. When the specific input signal is applied to the sample, the incident light is converged, and shows a focusing result, as Fig. 3- 6 illustrates.

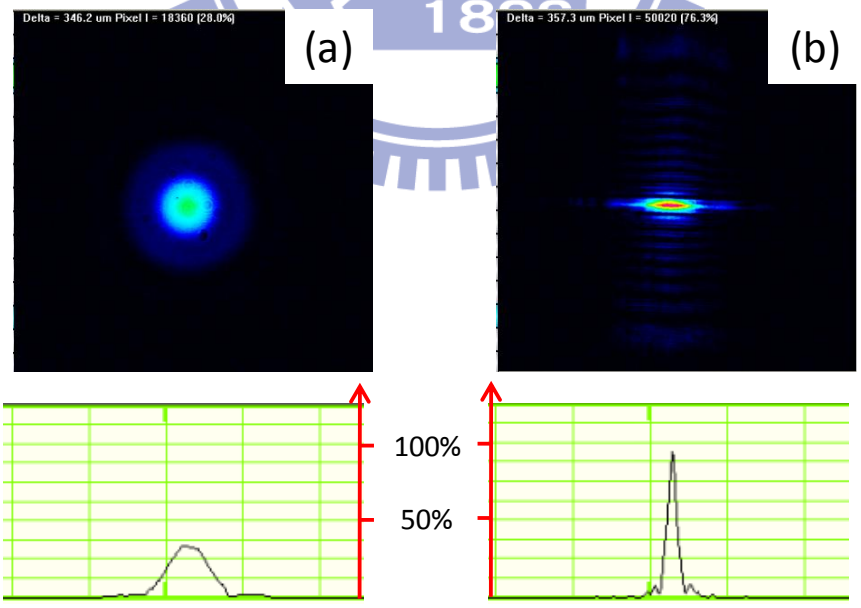

Fig. 3- 6 The focusing profile of LC Lens (a) no focusing effect, and (b) convex focusing effect

The interference pattern is one of the mostly used methods to measure the phase retardation of LC cells. To measure the interference pattern, an analyzer and a microscope have to be placed between the sample and the CCD camera in the measurement system. To evaluate the optical properties of LC Lens, we investigate the phase retardation by observing the interference pattern between the ordinary and extraordinary rays passing through the lens cell under crossed polarizers. The rubbing direction of the lens cell is oriented at 45° with respect to the fast axis of the linear polarizer.

3.2.2 Over-drive method

In LCD applications, over-drive method is wildly used for accelerating response times. With using optimized over driving voltages and switching to target operation, the LC response time can be much reduced.

In the study of LC lens, the device is usually designed to yield a larger optical power that means a thicker LC layer is requested (see 2.4.1). A thicker LC layer generally results a longer response time (see 2.4.2). For example, in conventional LC lens whose LC cell gap is 60 μm, the response time could reach 25 more seconds.

To minimize the response time issue, the over-drive method is utilized here. First, a large pulse is applied through the controlling electrodes to fasten response at the beginning of over-drive method. Next, the input signal is switched from large pulse to desired operating voltage to stabilize focusing effect [26]. This method is schematically illustrated in the following picture:

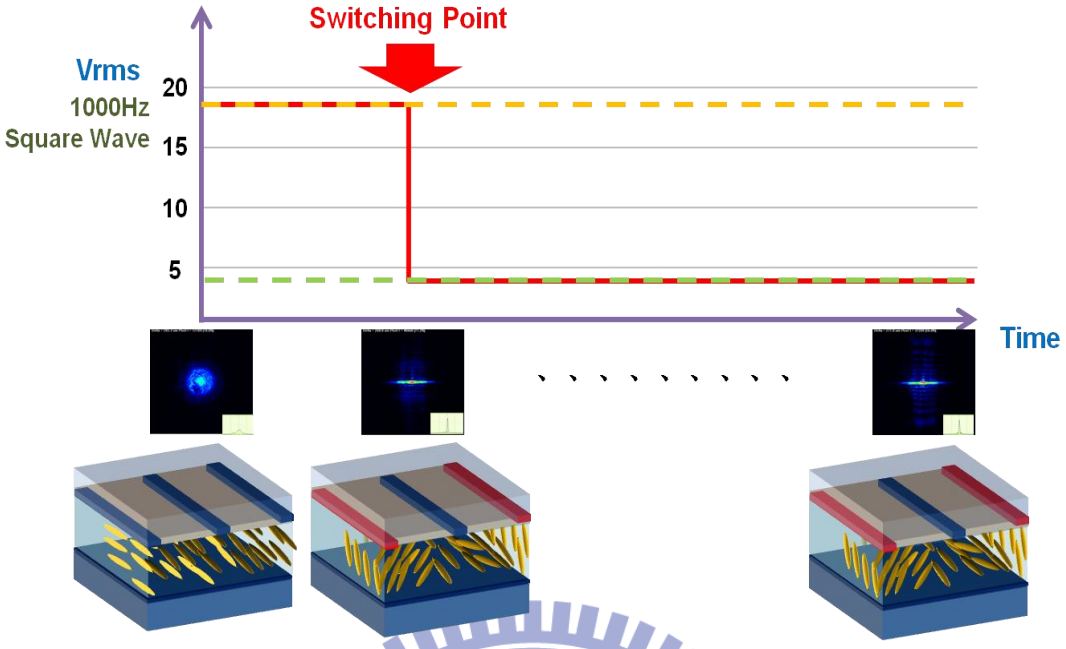

Fig. 3- 7 The schematic showing the concept of over-drive method. The red line, orange line, and green line represent applied voltage, Over-Drive voltage, and operating voltage respectively.

Generally speaking, applying a larger pulse at beginning of over-drive method can yield a shorter response time. Notice that too high electric energy could break the LC device.

Chapter 4

Electrode configuration design

The LC materials possess unique properties such as an electricity focal length (see 2.2). Therefore, the design of electrode configuration is crucial. In this chapter, two simulation tools to characterize the features of the LC lens are proposed. The commercial software 2DiMOS is used to model the LC deformations and the MATLAB is used to derive the refractive index distribution. Next, prior arts and the simulation model proposed by our group will be presented. Further, the discussion of the simulation result is also presented. Finally, the optimized electrode configuration is proposed after considering the issues in discussion.

4.1 Simulation tools

4.1.1 2DiMOS

The electro-optical calculator Display Modeling System (DIMOS^{TM}) developed by Autronic-MELCHERS GmbH was used to simulate the fringing field effect, the graphical user interface is as shown in Fig. 4- 1. 2DiMOS calculates the electro-optical properties of LCDs, and allows variations of the molecular orientation in two spatial dimensions so that lateral effects can be taken into account. All three elastic constants (K_{11}, K_{22}, K_{33}) and the natural are recognized for realistic simulations. The relaxation makes use of the rotational viscosityγ_1, hence, the dynamics of the LC director profile can be revealed. Besides, electrodes, dielectric layer and LC material layer are defined by polygons of arbitrary shape which is like in

a standard drawing application. The coupling capacitances of all electrodes can be calculated at arbitrary time levels. A voltage editor is included for the definition of various addressing schemes. Thus, the static and stationary electro-optical response as well as the dynamic behavior can be calculated.

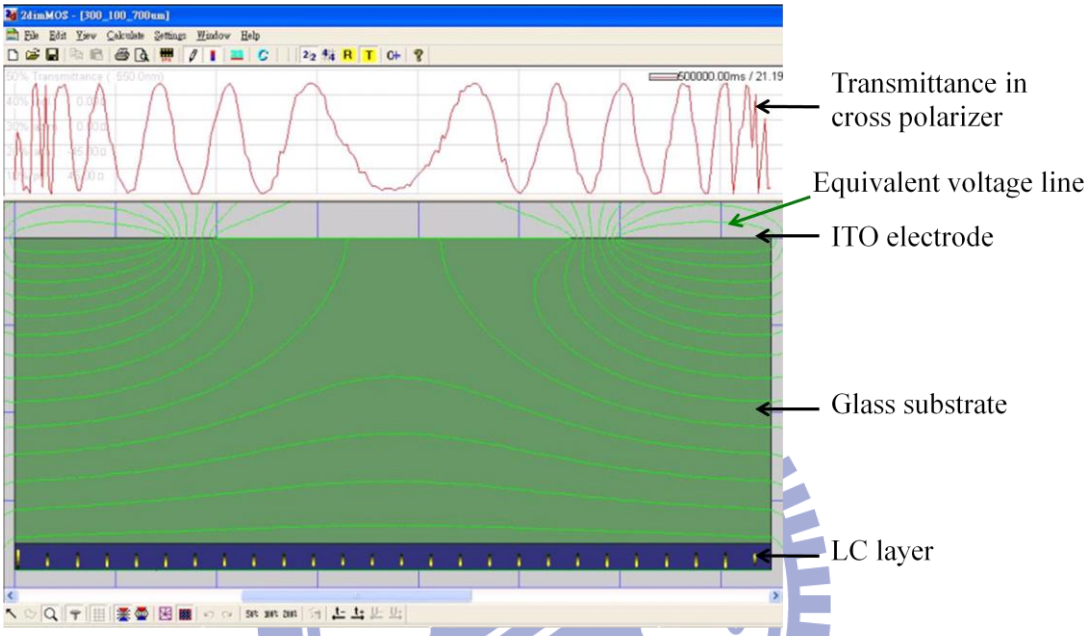

Fig. 4- 1 The graphical user interface of 2DiMOS

4.1.2 Evaluation of the lens structure

After editing the initial condition such as the applied voltage and specification of LC material and glass substrate, the LC director can be calculated by the 2DiMOS. These simulation results contain the polar and azimuthal angles of LC director which can be transformed into the refractive index by Eq.2-6. Therefore, the commercial software MATLAB has been used to program to transform the LC director into refractive index distribution. Based on the principle described in 2.4.1, the refractive index difference between the center and edge of the cell (Δn) and position along aperture is regarded as a smooth parabolic curve. However, when the geometry of the device structure or the boundary condition is not optimized yet, the refractive

index-radius distribution simulation result of LC director profile exhibits poor smooth gradient curve. Therefore, the Error Function (EF) is proposed to calculate the difference between the refractive index-radius distribution simulation result of LC director profile and the ideal parabolic curve to evaluate the focusing ability, as described following:

$$\mathbf{EF} = \sqrt{\frac{\sum_{i=i}^{aperture\_size}(S_i - P_i)^2}{aperture\_size}} \mathbf{x\ 100\%} \qquad \textbf{Eq. 4- 1}$$

where the S_i and P_i denote the simulated value and ideal value, respectively. P_i coordinates ideal quadratic function in whole aperture. The value of $(S_i - P_i)$ denote the difference between simulated and ideal result. Therefore, squaring this value eliminates the state of plus or minus value which has the same significant. Further, the squared value of every position is averaged. Finally, the Error Function is expressed in the percentage of the root of this averaged squared value. Briefly speaking, the lower EF value has smaller difference between the simulated and ideal results, which also represents the device structure in such boundary condition exhibits higher focusing ability.

4.2 Prior arts of double and multi-electrode LC lens

The design and fabrication of LC lens of some prior arts are based on the patterned electrode type LC lens because of simple geometry (see 1.2.2). The external electrode configuration is suggested if the size of lens' aperture is in millimeter, as shown in Fig. 4- 2. The LC material used here is E7 from Merck. Table 4- 1 shows the specification of E7.

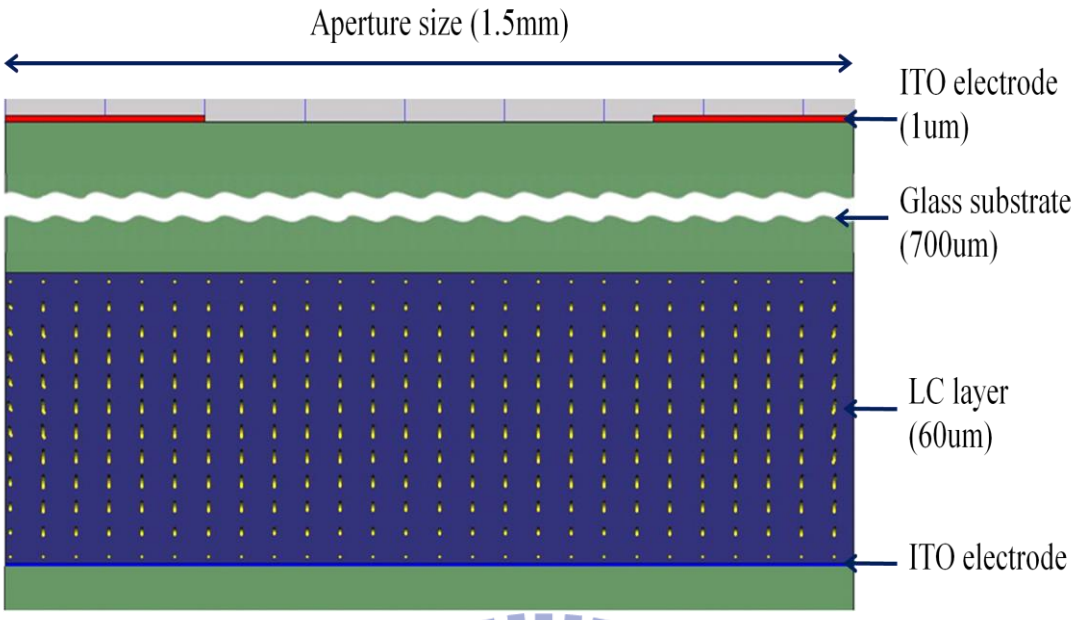

Fig. 4- 2 The configuration of our proposed LC lens

Items	Specification
Dielectric Constant of Glass Substrate	$\varepsilon_{glass} = 6.9$
The Specification of LC Material (Merck E7)	$K_{11} = 11.1$ pN
	$K_{22} = 5.9$ pN
	$K_{33} = 17.1$ pN
	$\gamma_1 = 233$ m Pa
	$\varepsilon_{\parallel} = 19.28$
	$\varepsilon_{\perp} = 5.21$
	$n_e = 1.7371$
	$n_o = 1.5183$

Table 4- 1 The simulation parameters for our proposed LC lens.

According to the Eq.2-10, the effective focal length is proportional to the cell gap of LC layer. The thicker cell gap of LC layer has shorter focal length. However, according to the Eq.2-13 and Eq.2-14, the response time is inverse proportional to the

cell gap of LC layer which means the thick cell gap of LC layer has slowly response time. The relationship between short focal length and response time is trade-off. Therefore, the suitable cell gap of LC layer is 60um and the shortest focal length which can be adjusted is about 4cm.

4.2.1 Simulation results of double-electrode LC lens

After setting up the device structure, the refractive index-radius distribution simulation result of LC director profile is yielded by assigning specific boundary condition. If the distribution of LC director is not smooth as a parabolic curve as shown in Fig. 4- 3, this device has poor focusing ability. In double-electrode configuration, the curve depicted with simulated result becomes disorder and far away from the ideal smooth parabolic curve when the operating voltage increases more than 30 volts. Moreover, the electric field distribution, which directly affects the LC director profile, cannot be adjusted due to the low freedom of adjustment in the electrode configuration.

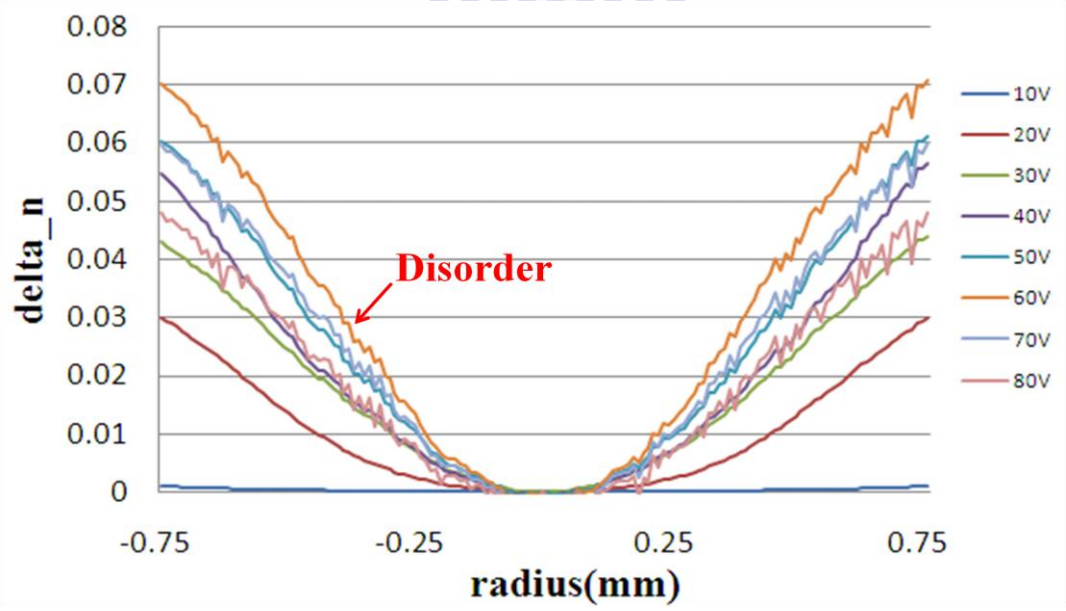

Fig. 4- 3 The distribution of Δn of double-electrode structure

Further, the relationship between operating voltage and focal length is not linear, and the maximum Δn value is obtained when the operating voltage is 60 volts. However, this Δn value is still not large enough which means the focal length is very long. As the applied voltage increased over 60 volts, the maximum Δn value cannot be increased, because the LC director will follow the electric field and almost perpendicular to the electrode plane in the large applied voltage. Therefore, the difference of LC director between the center and edge cannot be varied by increasing applied voltage.

In order to generate a high optical performance LC lens including high focusing ability and short focal length, the multi-electrode driven structure was proposed. Since multi-electrode driven structure has high freedom of adjustment, the refractive index distribution can be adjusted to modify parabolic curve and has large Δn distribution value.

4.2.2 Simulation results for multi-electrode driven LC lens

The step of optimizing electrode configuration is shown in Fig. 4- 4. First of all, the simulated result curve was fitted with the ideal parabolic curve through adjusting the number of electrode slit. We investigated the optimized electrode number by investigating the Error Function. The ratio of W_E/W_S was fixed at 1 at the beginning step, where W_E and W_S denote the electrode width and slit width respectively. The simulation result shows the optimized electrode number is 9, as shown in Fig. 4- 5.

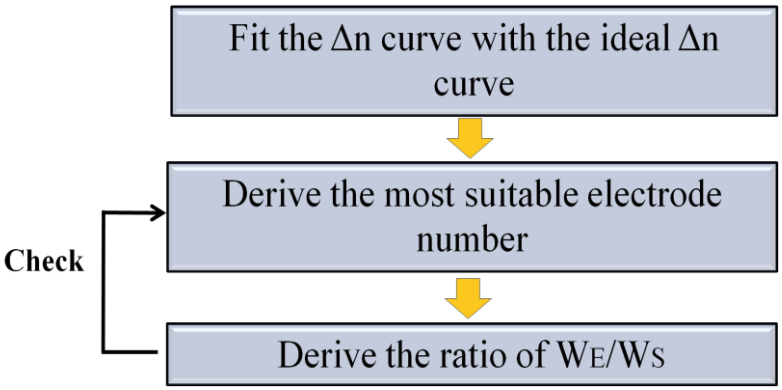

Fig. 4- 4 Flow chart of the simulation steps

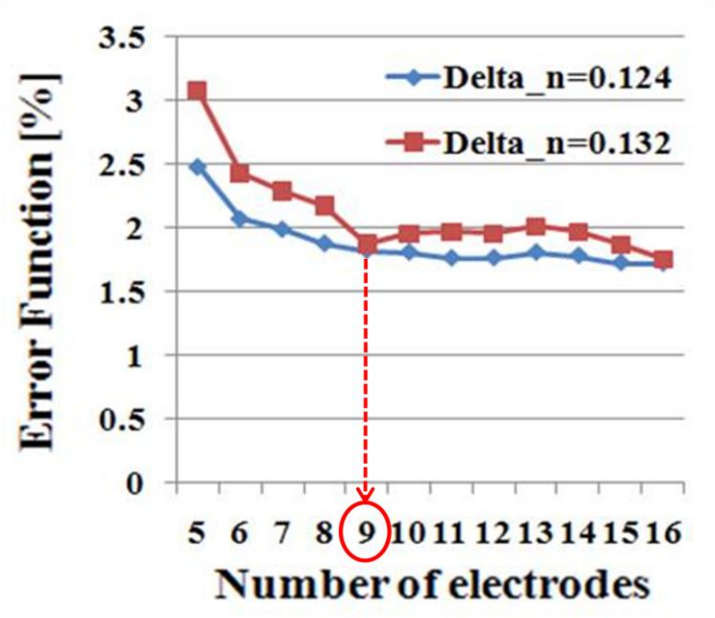

Fig. 4- 5 Simulation result of error function with electrode number

After optimizing the electrode number which was set as 9, the optimized ratio of W_E/W_S was investigated by minimizing the value of Error Function. The simulation result shows the most suitable ratio of W_E/W_S is 1, as shown in Fig. 4- 6. Therefore, the optimized electrode number and W_E/W_S in multi-electrode driven LC lens are 9 and 1 respectively. Fig. 4- 7 shows the refractive index-radius distribution simulation result of LC director profile in multi-electrode driven LC lens. The simulation result curve is smooth and is barely different with the ideal parabolic curve. In conclusion, MeDLC performs high focusing ability.

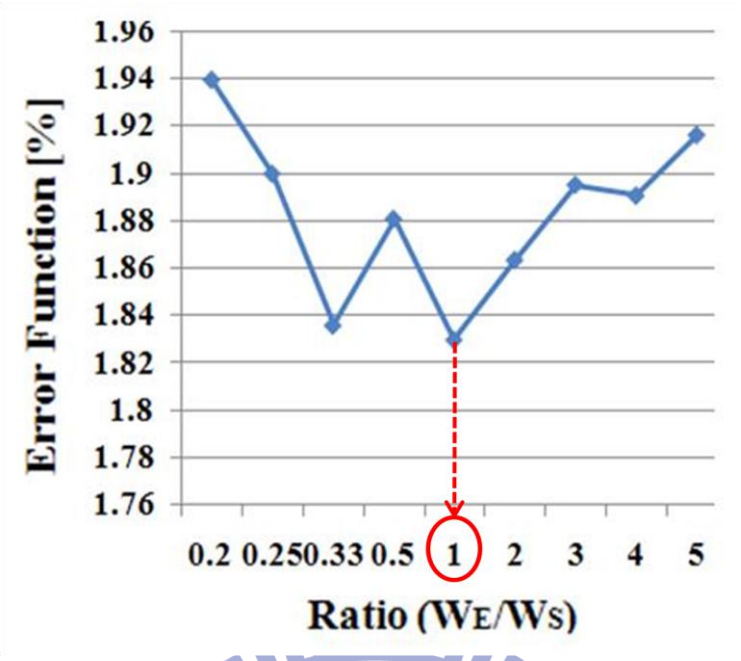

Fig. 4- 6 Simulation result of error function with Ratio of WE/WS

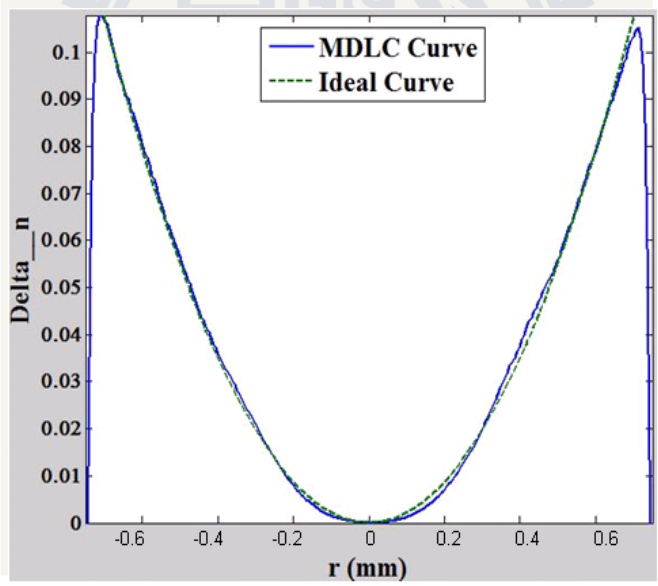

Fig. 4- 7 Simulation result of MeDLC structure

Though the MeDLC improves focusing performance compared with conventional double-electrode LC lens, the requirements for operating voltage and response time are insufficient. Therefore, a modal control using a triple electrode set is proposed to reduce operating voltage and response time simultaneously.

4.3 Gradient driven LC lens

To yield a superior electrical field in LC layer, a well-designed structure with external electrode is suggested, as mentioned in 4.2. After improving the focusing ability with proposed MeDLC, the response time is still long and the operating voltage is still high. To overcome these two issues, our previous simulation work indicated the configuration with internal continuous-distributed electrode has the ability to achieve a gradient electrical field distribution and to maintain the energy inside the LC layer simultaneously. These two features not only yielded the gradient phase retardation, but also sufficiently employed the applied energy. Fig. 4- 8 shows the structure for achieving these two features. The similar concept, LC lens with Modal Control, was proposed by A. F. Naumov et al. As mentioned in 1.2.2, a high resistance material which generally has ~ 1-10 M/□ sheet resistivity was utilized as the control electrode, and a thin LC layer was used to create a smooth gradient electric field distribution. However, the numerical aperture (NA) was relatively low due to the small optical power, although the operating voltage is low (~10V_{rms})

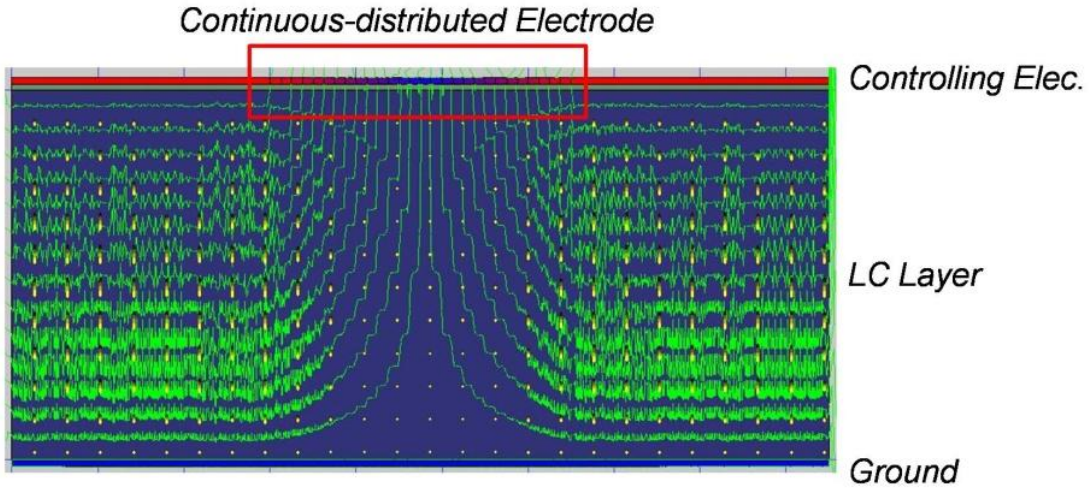

Fig. 4- 8 The structure of internal continuous electrode performs a smooth gradient electrical field and can conserve the electrical energy inside the LC layer.

To achieve the configuration as shown in Fig. 4- 8, Gradient Driven Liquid Crystal Lens (GD-LC Lens) was proposed to intrinsically solve the issues of slow focusing and high operating voltage. GD-LC Lens utilized a high resistance layer (high R layer) to be the internal continuous-distributed electrode to achieve low operating voltage and improve the focusing time simultaneously [27]. Experiments for testing the properties of the high R layer were investigated. In the testing device, the high R layer, which was spin coated on a substrate, connected two controlling electrodes, as shown in Fig. 4- 9. This structure generated gradient electric field distribution when there were two different operating voltages applied on each controlling electrode. Clevious P whose specification was shown in Table 4- 2 was chosen to be the high R layer. A 60μm cell gap of LC molecule, E7 (Δn=0.2) from Merck, was aligned in anti-parallel with controlling electrodes. The two controlling electrodes in the testing device were separated by 2mm. In the investigation of spatial phase retardation, different operating voltages driven at 1 kHz were applied to the right controlling electrode in the testing

device. The left controlling electrode in the testing device was ground connected to yield a potential difference (ΔV) between two controlling electrodes. Different interference pattern were observed by adjusting operating voltage. At $V=3V_{rms}$, the interference pattern was denser on the right side, as shown in Fig. 4- 10(a). This pattern indicates a convex lens effect can be achieved by symmetrically combining two identical structures with the same operating voltage. On the other hand, at $V=5V_{rms}$, the interference pattern was denser on the left side, as shown in Fig. 4- 10(c). A concave lens effect also can be realized by adjusting the driving method.

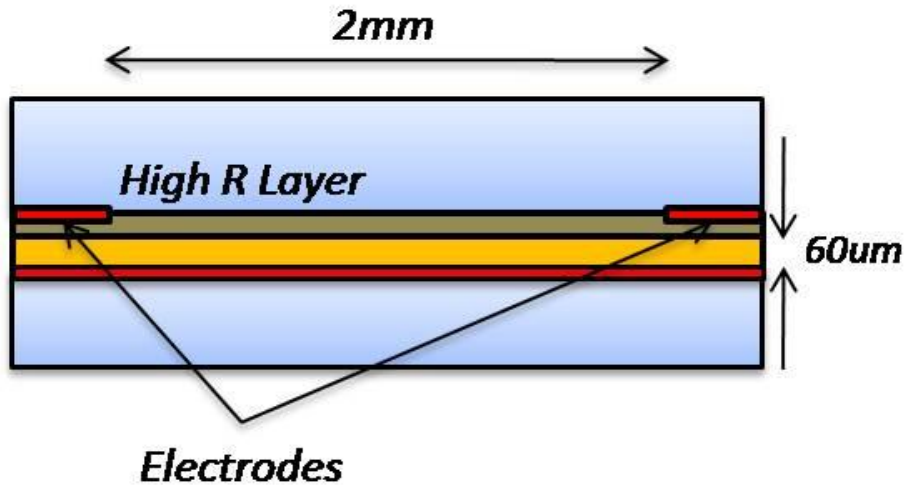

Fig. 4- 9 The testing device of LC cell with high resistance layer connected by two controlling electrodes.

Specification of Clevious P	
Chemical Characteristics	
Sodium	Max. 500 ppm
Sulfate	Max. 80 ppm
Physical Characteristics	
Solid content	1.2 ~ 1.4 %
Viscosity	60 ~ 100 mPa · s
pH-value	1.5 ~ 2.5
Surface resistance	Max. 1 M ohm
Informative Technical Data	
Conductivity	Max. 10 S/m (depending on the type of coating formulation)
Density at 20℃	1.003 g/cm^3
Mean particle size	Approx. 80 nm (size of the swollen gel particles)
Refractive index at 589nm	1.5228
Surface tension at 20℃	71 mN/m

Table 4- 2 The specification of Clevious P

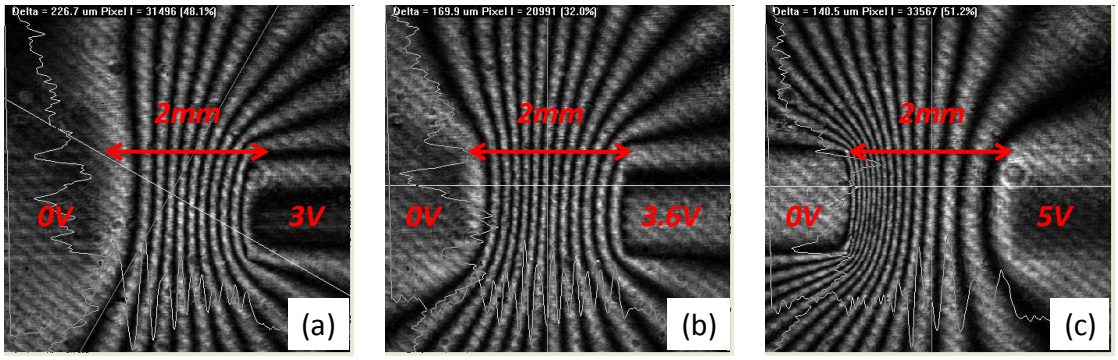

Fig. 4- 10 The results of interference pattern of the testing device driven by different operating voltages, (a) ΔV=3 Vrms, (b) ΔV=3.6 Vrms, and (c) ΔV=5Vrms. The LC cell was design by 60μm cell gap driven by the two controlling electrodes with 2mm separation.

According to the testing results, the structure of GD-LC Lens was constructed combining the triple internal electrode set and the high resistance layer. Three controlling electrodes included two marginal controlling electrodes and a central controlling electrode. The lens aperture was 2mm wide and the LC cell gap thickness was 60μm. The thickness of glass substrate was 0.4mm.

By applying the operating voltage through the marginal electrodes and ground connecting the central electrode, GD-LC Lens works in convex mode. Oppositely, by applying the operating voltage through the central controlling voltage and ground connecting the two marginal electrodes, the GD-LC lens works in concave mode. The arbitrary electric field gradient profile was achieved by adjusting driving voltages. The structure is shown in Fig. 4- 11.

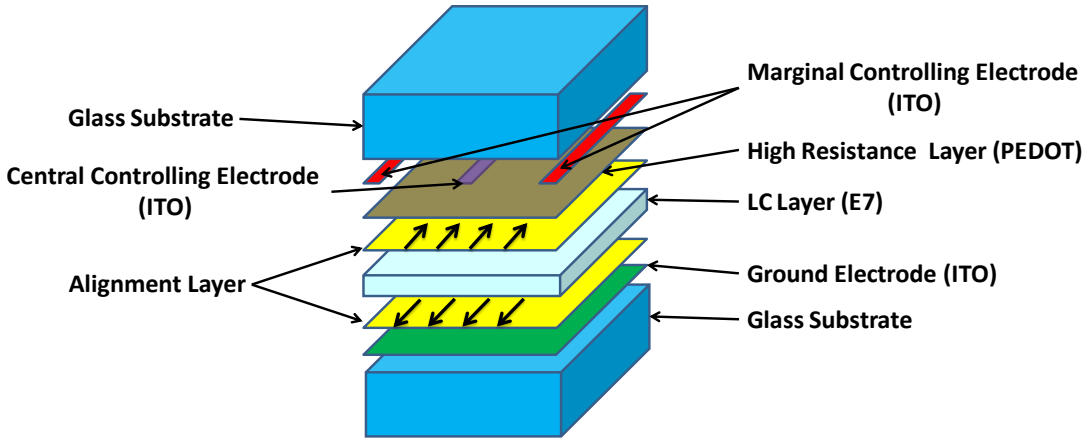

Fig. 4- 11 The configuration of GD-LC Lens. The structure with 2mm lens aperture and 60um anti-parallel LC cell gap was constructed combining combining the triple internal electrode set and the high resistance layer.

4.4 Summary

In this chapter, the simulation model to optimize the electrode configuration and boundary condition is presented. The MeDLC lens which has optimized focusing performance among external type electrode configuration was proposed. In order to reduce slow focusing and high operating voltage issues, the GD-LC lens was proposed. Moreover, this GD-LC lens can be operated in convex and concave mode by reversing the driving method.

Chapter 5

Experimental result and discussion

After ensuring the optimized structure, the optical performance of device is fabricated and measured with using measurement system in 3.2.1. Fig. 5- 1 shows the image of cylindrical type GD-LC lens device. In this chapter, the focusing profile, phase retardation, and the focusing time which are critical properties of GD-LC lens will be presented.

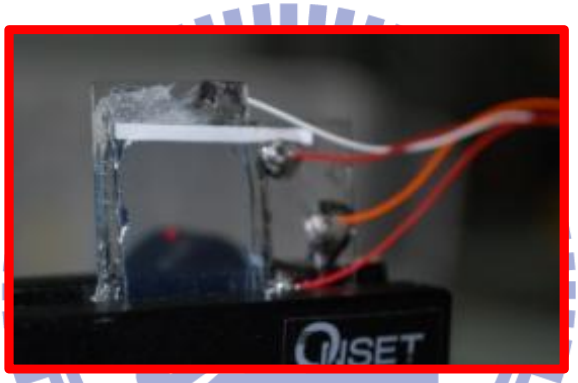

Fig. 5- 1 The cylindrical type GD-LC lens

5.1 Electricity dependent focal length

Focal length of the GD-LC Lens is tunable and voltage dependent. As operating voltage increased, the focal length became gradually shorter. Fig. 5- 2 shows the relationship between focal length and operating voltage. The LC cell gap was designed as 60μm and the operating voltage was generally lower than $6V_{rms}$. The shortest focal length was not estimated due to the limitation of the measurement system and the CCD sensor's structure.

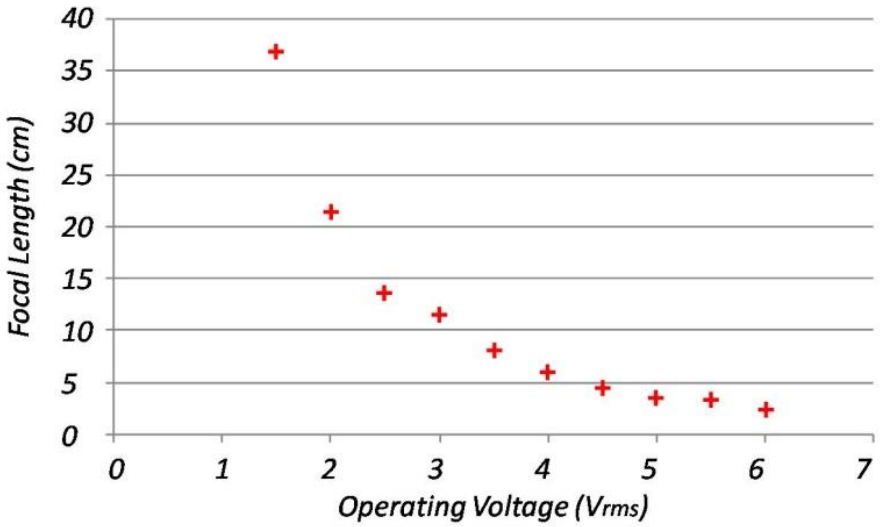

Fig. 5- 2 The relationship between the focal length and the operating voltage of GD-LC Lens. The focal length was tunable from infinity to 3.5cm only driven by less than 6Vrms operating voltage.

5.2 Phase retardation

The interference pattern is one of the mostly used methods to measure the phase retardation of LC cells. To evaluate the optical properties of GD-LC Lens, we investigated the phase retardation by observing the interference pattern between the ordinary and extraordinary rays passed through the device under crossed polarizers. The rubbing direction of the lens cell is oriented at 45° with respect to the fast axis of the linear polarizer. Two images of GD-LC Lens driven in convex and concave modes are shown in Fig. 5- 3(a) and Fig. 5- 3(b) respectively.

In convex mode, as shown in Fig. 5- 3(a), GD-LC Lens yielded a phase retardation approximating to that of ideal lens with 1.6mm effective lens aperture. This result which is derived in Eq.2-10 was coherent to 5.1.

On the other hand, the ground connected central electrode with two voltage applied marginal controlling electrodes drive GD-LC Lens in concave mode. The

result presented the phase retardation is much closer to that of an effective ideal lens, as Fig. 5- 3(b) illustrated.

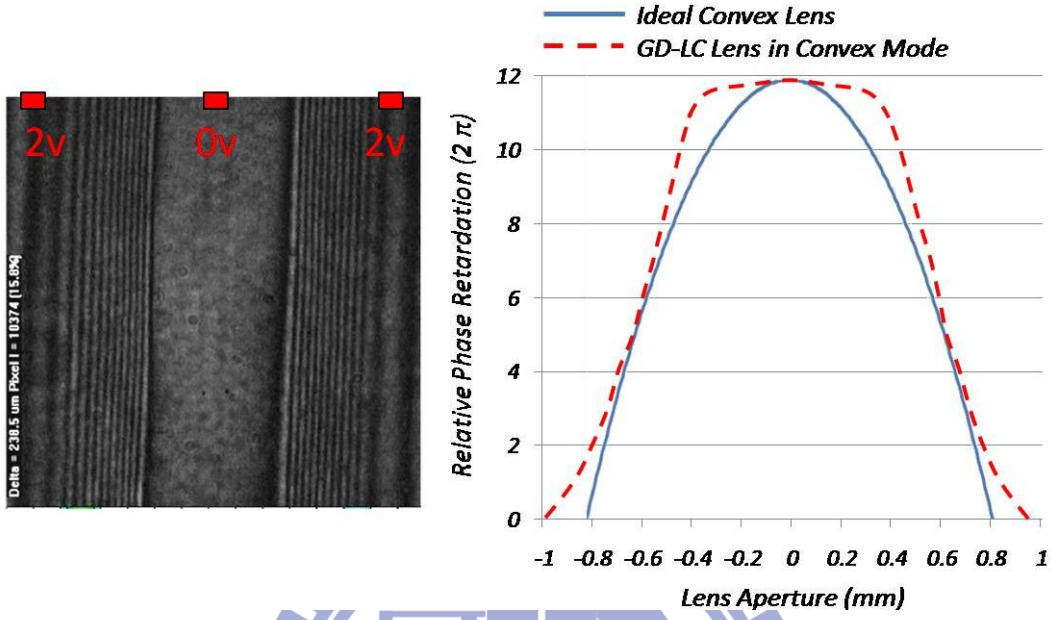

(a)

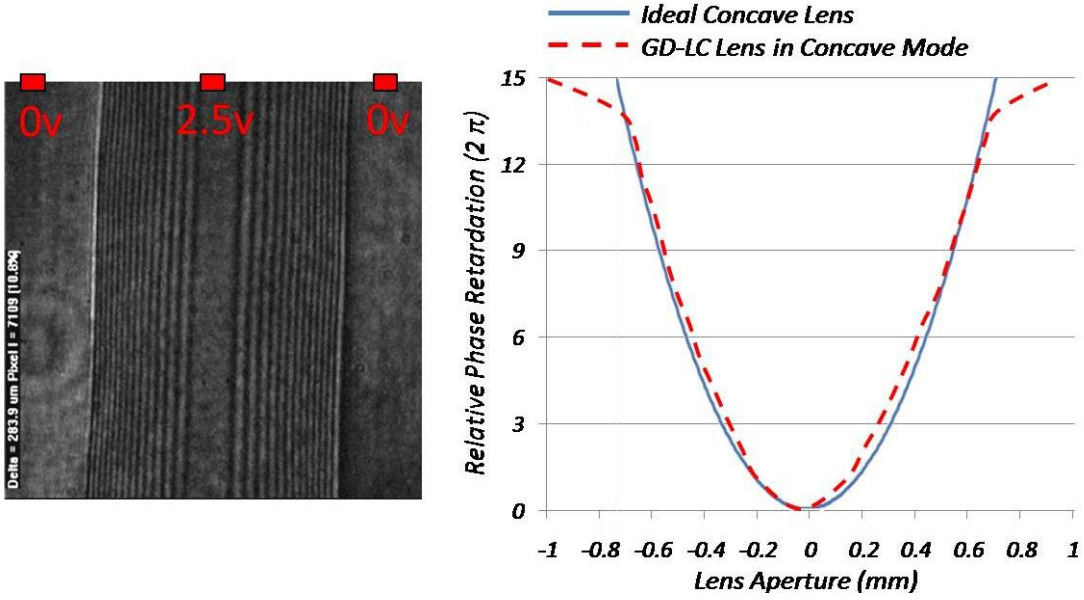

(b)

Fig. 5- 3 The phase retardation of GD-LC Lens operated in (a) convex, and (b) concave modes. By the different operating arrangement, both convex and concave lenses were achieved.

Compared with concave mode, the profile in convex mode was not significantly controlled due to the low controlling freedom. In fact, the LC molecular near the zero-volt controlling electrode obtained inadequate driving voltage to response. This phenomena resulted a quite large area maintained the same phase retardation near the zero-volt controlling electrode which actually decreased the focusing quality. To minimize the difference between the estimated phase retardation curve and the ideal parabolic curve, two approached are suggested: The first approach is to input a driving voltage higher than zero volt, for example: 1 volt, through those zero-volt controlling electrode so that the LC molecular near those zero-volt controlling electrodes may obtain adequate driving voltage to response. The second approach is to place more controlling electrodes inside the aperture to elevate the freedom of controlling.

5.3 Focusing time

The focusing process with respective focusing time of GD-LC Lens and the conventional LC lens with internal electrodes were recorded as shown in Fig. 5- 4. All the structures were designed with the same parameters, only the different configuration of controlling electrodes were compared. For GD-LC Lens, the result shows an instantaneous focusing within 0.2 sec by $3.5V_{rms}$ stable operating voltage with using only less than $15V_{rms}$ Over-drive voltage. This result shows a feasible range for commercial products and many applications utilizing LC lenses. Compare to the conventional LC lens whose initial focusing time was unpractical required around 25sec driven by ~$25V_{rms}$ stable operating voltage.

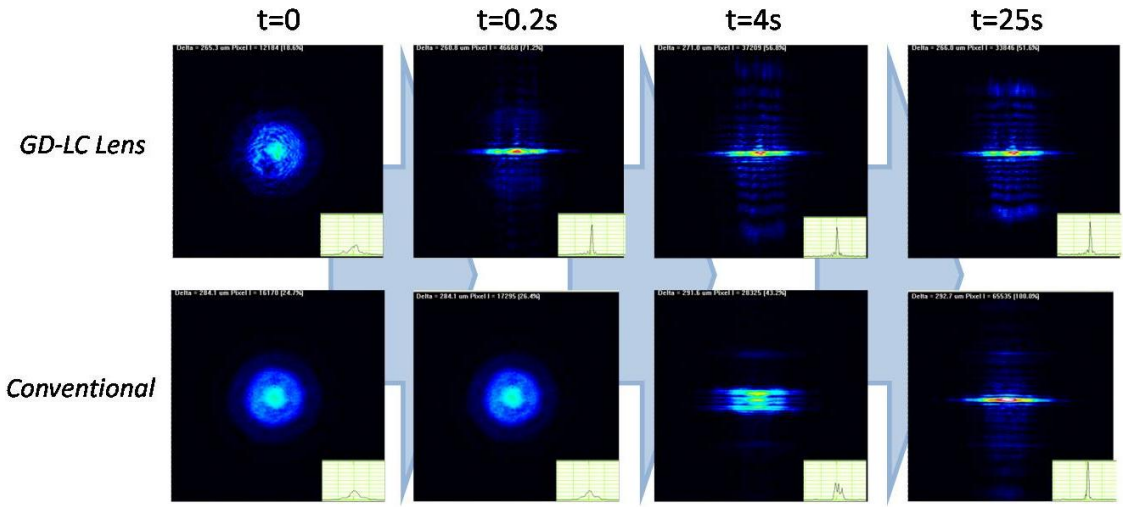

Fig. 5- 4 The focusing process of GD-LC Lens and the conventional LC lens with internal electrodes. In GD-LC Lens, the light was focused within 0.2 seconds and stabled after 0.2 seconds. On the other hand, the focusing time of the conventional LC lens was approximately 25 seconds.

Enlarging the Over-drive voltage may much decrease the focusing response time less than 0.2 second. However, the focusing response time shorter than 0.2 second was unable to be exactly estimated due to the minimum frame rate of the CCD camera is 0.2 second. On the other hand, a too high Over-drive voltage, for example: 40 volt, may break the electrical properties of the GD-LC lens. The affects of GD-LC lens under too high Over-drive voltage were not completely estimated so far.

Table 5- 1 shows the summary of comparison between GD-LC Lens and conventional LC lens with internal electrodes. Overall speaking, GD-LC Lens dramatically improved 99.3% focusing time and reduced 86.0 % operating voltage.

Comparison	*LC cell Gap*	*Operating Voltage*	*Focusing Time*
GD-LC Lens	*60 μm (E7)*	*3.5 V_{rms}*	*0.2 s*
Conventional LC Lens with Internal Electrodes	*60 μm (E7)*	*~25 V_{rms}*	*25 s*

Table 5- 1 The comparison of focusing time and corresponding operating voltage. The result shows GD-LC Lens significantly improved the focusing time and only driven by low operating voltage.

5.4 MTF

The module transfer function (MTF) was introduced to evaluate the focusing quality of GD-LC lens. Different sinusoidal wave were convolved with the point spread function to generate a transfer function on the image plane, as shown in Fig. 5-5. The maximum and minimum values of the transfer function were investigated to obtain the MTF value, as shown in Eq.5-1 [28][29].

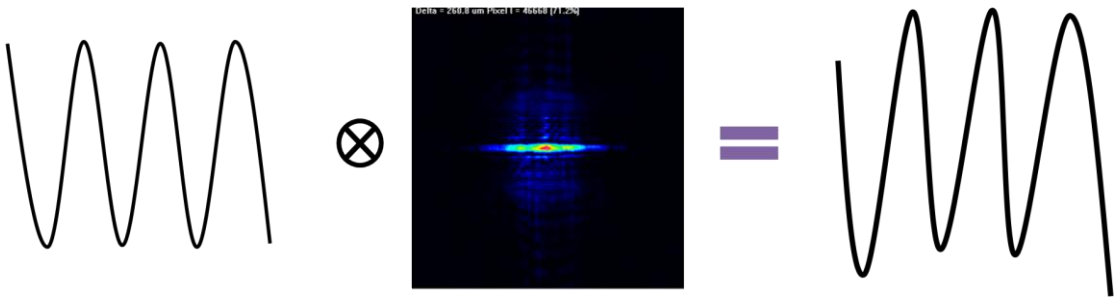

Fig. 5- 5 Transfer function is obtained convolving sinusoidal wave and the point spread functionl.

$$\mathbf{MTF} = \frac{\mathbf{Max(transfer\ function) - min(transfer\ fuction)}}{\mathbf{Max(transfer\ function) + min(transfer\ function)}} \qquad \textbf{Eq. 5- 1}$$

The MTF value of GD-LC lens is decreased as spatial frequency increasing and dropped to almost zero when the spatial frequency is higher than 20 cycle/mm, as shown in Fig. 5- 6. This result was reasonable because the full width at half maximum of the focusing profile was about 50um. The minimum MTF of GD-LC lens was slightly higher than zero because the estimated minimum intensity was not level shifted. The ideal MTF value was calculated and also shown in Fig. 5- 6 [30].

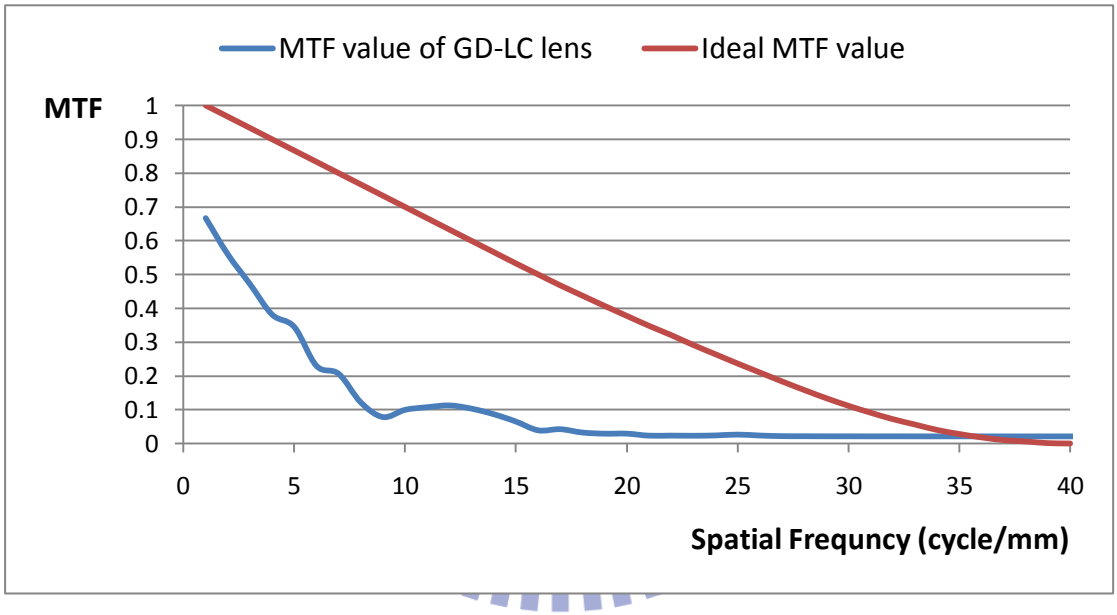

Fig. 5- 6 The blue line represented the MTF value of cylindrical type GD-LC lens. The red line represented the ideal MTF value. The aperture size was 2mm. The resolution of the CCD was 50 cycle/mm.

Obviously, the focusing quality of GD-LC lens was insufficient which was corresponded with the discussion of the result in phase retardation profile. Besides, minimizing the full width at half maximum of the focusing profile is also critical to promote the focusing quality. Two approaches are suggested: First is increasing the operating voltage in zero-volt controlling electrode to reducing the area maintaining the same phase retardation so that a sharper focusing profile can be obtained. Second

is minimizing the area of the central controlling electrode. In fact, the LC molecular under the area of controlling electrode obtained the same driving voltage to response. Therefore, minimizing the area of the central controlling electrode allows a larger portion of LC in the aperture to perform either convex or concave effect which keeps a higher freedom of controlling.

5.5 Improvement in Focusing Quality

Obviously, the focusing quality needs to be improved from the perspective of the MTF result. Some methods to improve the focusing quality were proposed in previous section and can be classified: First, adjust the operating frequency to obtain the desired phase retardation distribution. Second, increase the amplitude of input signal through the central controlling electrode or minimize the area of the controlling electrodes so that the active region of the lens aperture can increase. However, to adjust the driving method is much simpler and more convenient than to rearrange the structure condition. Thus, only the improvement through adjusting driving method will be demonstrated as follows.

The physical properties of modal control type LC lens were introduced in 2.5. Beside amplitude, the phase retardation distribution in GD-LC lens is also attributed to operating frequency. Thus, the interference pattern results for different operating frequency were recorded to investigate its influence on the phase retardation distribution. The operating voltage was 3.2 volt. The operating frequency was altered from 1kHz to 100kHz. Only convex results were demonstrated, as shown in Fig. 5- 7. As the operating frequency increased, the impedance constructed by the high resistance layer and LC increased so that the operating voltage dropped faster between

the marginal and central controlling electrodes which resulted in the interference pattern became condensed to marginal controlling electrodes.

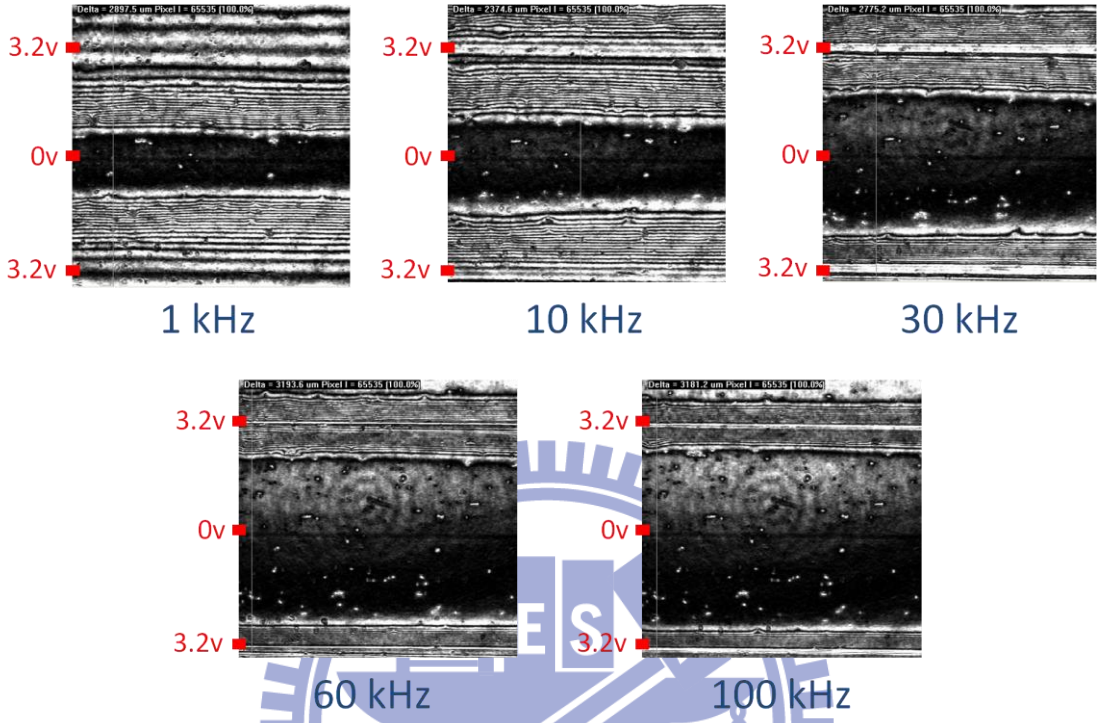

Fig. 5- 7 The interference pattern results for difference operating frequency. The red dot denotes the position of controlling electrodes.

To further improve focusing quality, adjusting the operating voltage distribution across the lens aperture is necessary. Fig. 5- 8 shows the interference pattern result and its corresponded focusing profile after adjusting the operating voltage distribution across the lens aperture which can be achieved by tuning the operating frequency or the operating voltage on the controlling electrode. The operating voltages were 3.2 volts and 0.72 volts on the marginal and central controlling electrode respectively. The operating frequency was 5 kHz. The corresponded MTF value was also calculated and shown in Fig. 5- 9. Apparently, the focusing quality was promoted after adjusting the driving method from the perspective of MTF results.

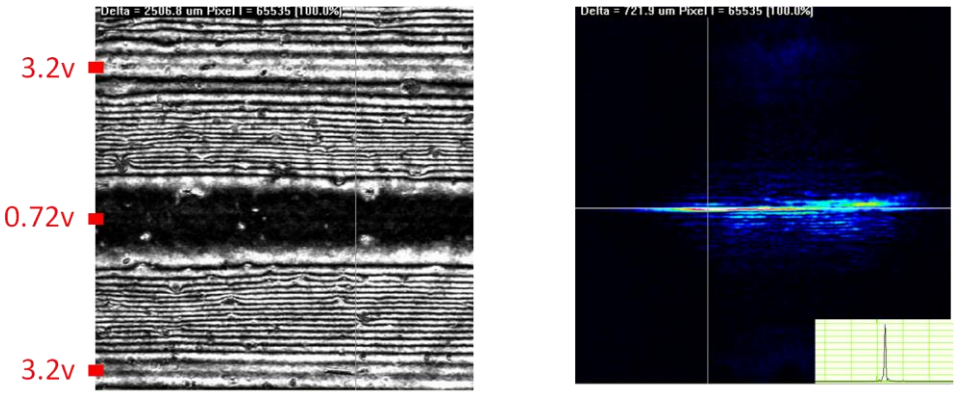

Fig. 5- 8 The interference pattern result (left) and its corresponded focusing profile (right) after adjusting the operating voltage distribution. The red dot denotes the position of controlling electrodes.

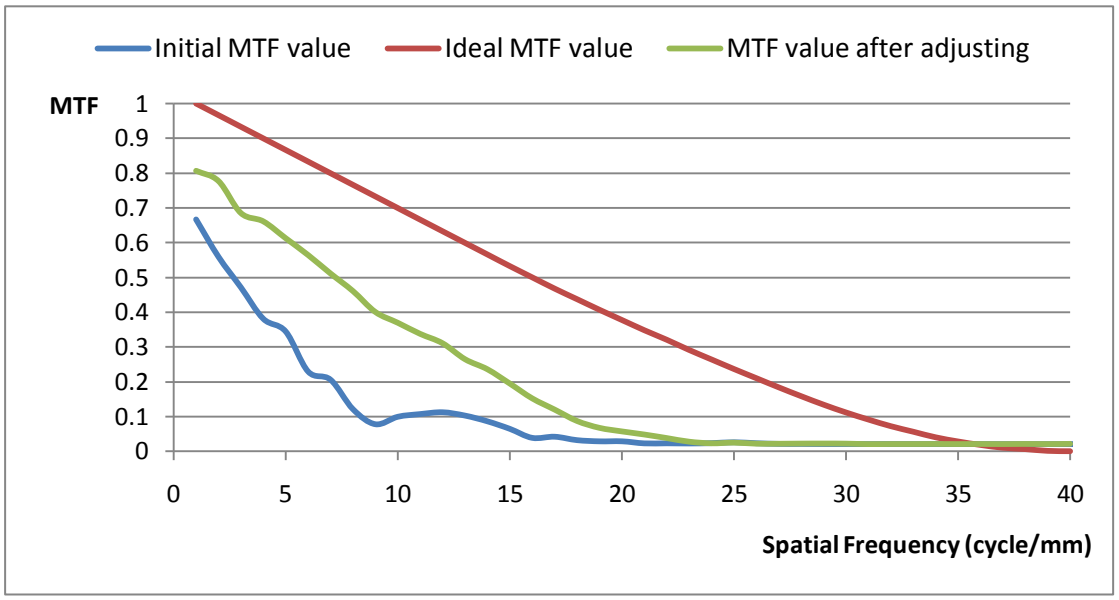

Fig. 5- 9 The MTF value of the GD-LC lens. The blue line, red line, and green line represent the initial MTF value, the ideal MTF value, and the MTF value after adjusting of the GD-LC lens respectively.

Chapter 6

Conclusion and future work

6.1 Conclusion

The tunable lens has been widely used in optical systems and other electro-optic devices. To tune the focal length, the conventional tunable lenses require large space to move lens mechanically. However, the LC lens which has electricity dependent focal length requires no moving mechanical part. Therefore, the LC lens is smaller and lighter than the conventional tunable lenses to be practical application restricted with compact volume.

To promote the focusing ability of LC lens, the MeDLC lens was proposed. 9 electrodes with $W_E/W_S=1$ is the optimized structure determined by using simulation model. Although the MeDLC lens provide high focusing ability, the long focusing time and high operating voltage issues need to be improved. Therefore, the GD-LC lens exhibiting fast focusing response with using low operating voltage was proposed. The LC cell gap was 60 um and the lens aperture was 2mm. The focal length was electrically tunable from infinity to 3.5cm only driven by less than $6V_{rms}$. The focusing time was dramatically improved to 0.2sec with using Over-drive Method. Compared with result for conventional LC lens, the regular focusing time is 25 more seconds and extremely high driving voltages is necessary, GD-LC Lens brought the applications utilizing LC lenses to be feasible and practical. Moreover, both convex and concave lens effect were achieved in GD-LC Lens with adjusting different driving method. The focusing quality issue was discussed and some approaches to promote the focusing

quality were demonstrated. In conclusion, GD-LC Lens would be potentially used for camera phones, time sequential auto-stereoscopic 3D display and other tunable-focus optics application.

6.2 Future work

Although the GD-LC lens performs ultra fast response with low operating voltage, the focusing quality is insufficient. Beside the proposed methods in 5.5, in the future our group will try to combine the concepts of MeDLC, Over-Drive method, and GD-LC lens to yield a high quality, high response speed, and low power LC lens, as shown in Fig. 6- 1.

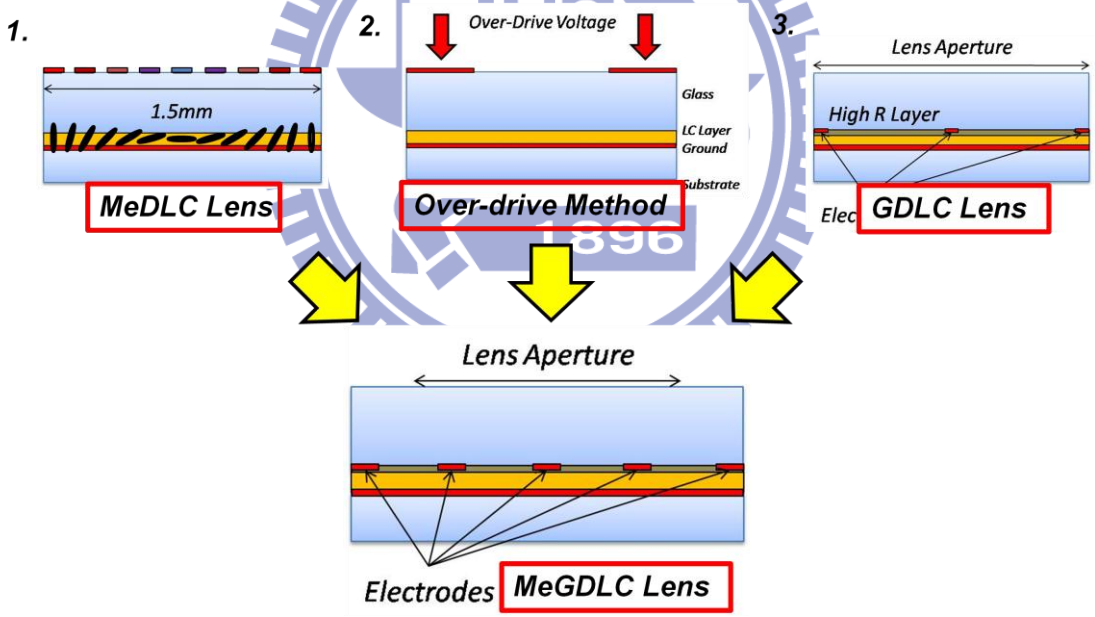

Fig. 6- 1 Combine the advantages of each proposed technology to yield a high quality, high response speed, and low power LC lens.

In fact, the circular type GD-LC lens was fabricated few months ago, as shown in Fig. 6- 2. However, all the samples of circular GD-LC lens became invalid after period of storage. The pattern in the top substrate should be redesigned in the short future.

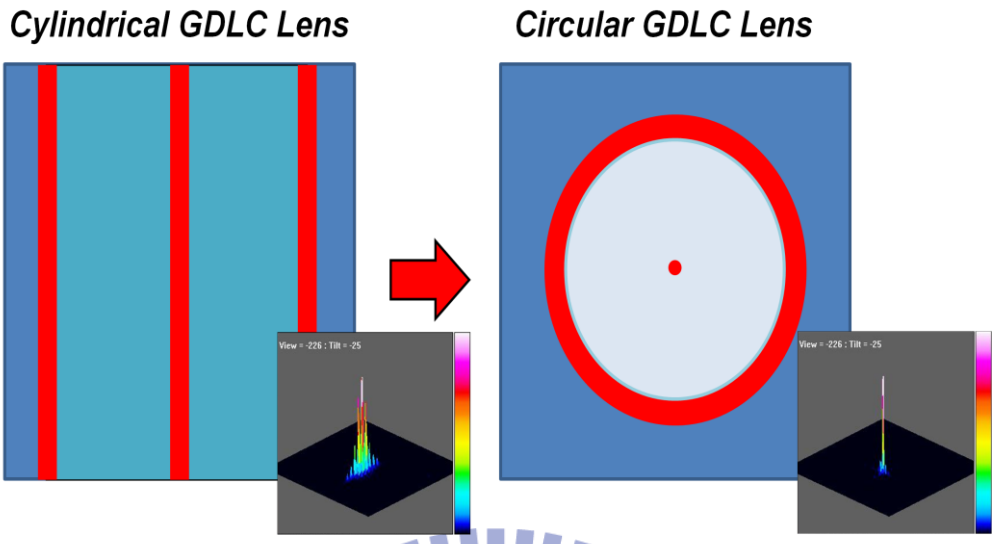

Fig. 6- 2 The circular GD-LC lens was fabricated and studied for lens-head applications.

Besides, by using LC lens to capture different depth of focusing in one focusing response, complete depth information of the image can be obtained, as shown in Fig. 6- 3.

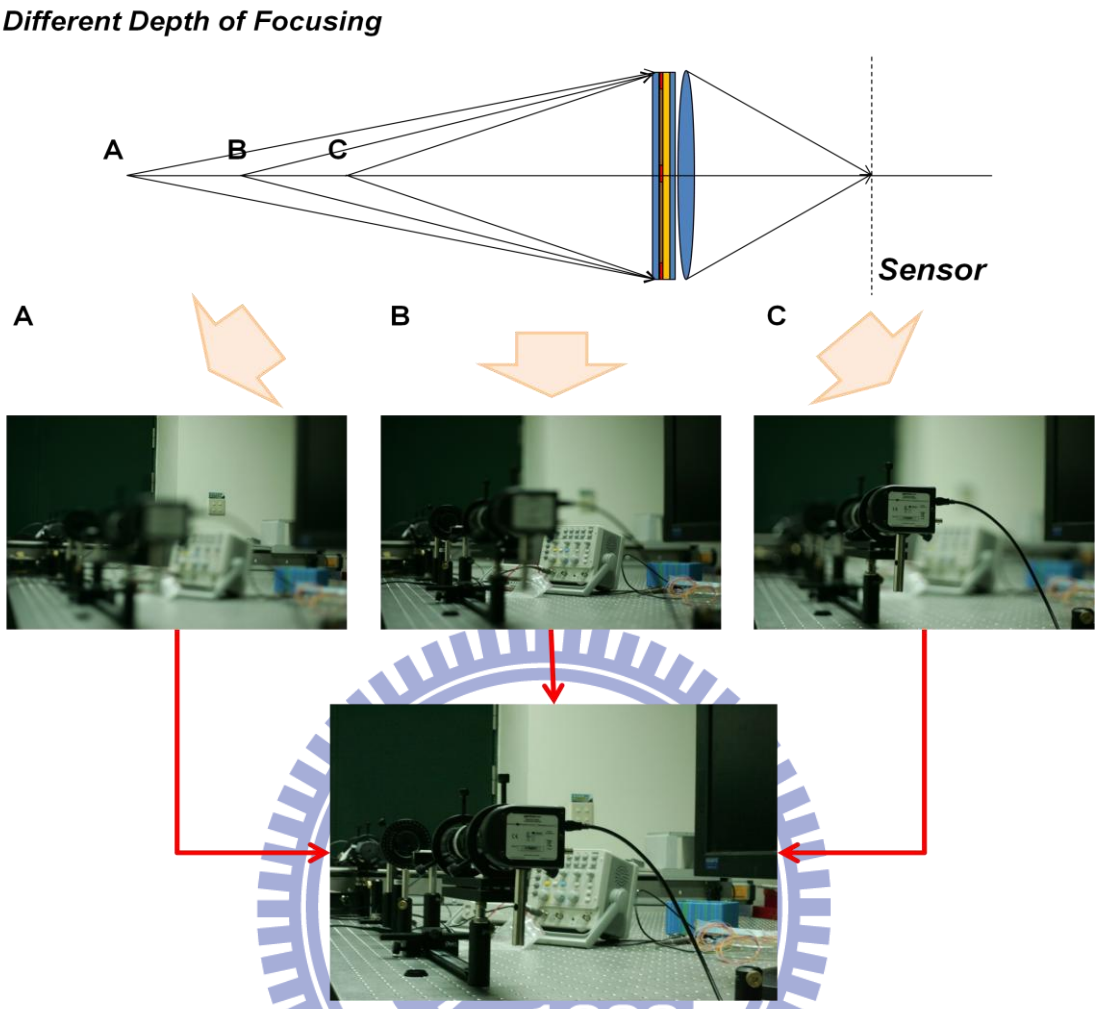

Fig. 6- 3 Capture different depth of focusing in one focusing response for 3D imaging applications.

Reference

[1] H. Ren, Y.H. Fan, Y. Lin, and S.T. Wu, SPIE's oemagazine (2004)

[2] http://en.wikipedia.org/wiki/Zoom_lens

[3] S. Kuiper, and B. H. W. Hendriks, "Variable-focus liquid lens for miniature cameras", Appl. Phys. Lett. Vol. 85 No. 7 p.1128-1130 (2004)

[4] H. Ren, and S. T. Wu, "Variable-focus liquid lens", OPTICS EXPRESS, Vol. 15 No. 10 (2007)

[5] S. Sato, "Liquid-Crystal Lens-Cell with Variable Focal Length", J. J. Appl. Phys. Vol.18 No.9 pp.1679-1684 (1979)

[6] T. Nose, M. Honma, and S. Sato, "Influence of the Spherical Substrate in the Liquid Crystal Lens on the Optical Properties and Molecular Orientation State", SPIE Vol.4418 (2001)

[7] S. Sato, "Application of Liquid Crystal to Variable-Focusing Lenses", OPTICAL REVIEW Vol.6 No.6 (1999)

[8] A. F. Noumov, and M. Yu. Loktev, "Liquid-crystal adaptive lenses with modal control", OPTICS LETTERS, Vol. 23 No. 13 p. 992-994 (1998)

[9] B. Wang, M. Ye, M. Honma, T. Nose, and S. Sato, "Liquid Crystal Lens with Spherical Electrode", J. J. Appl. Phys. Vol.41 pp.1232-1233 (2002)

[10] H. Ren, and S.T. Wu, "Adaptive liquid crystal lens with large focal length tunability", OPTICS EXPRESS Vol. 14 No.23 p. 11292-11298 (2006)

[11] http://www.cellular-camera-phones.com/camera-cell-phones.html

[12] http://www.guardian.co.uk/technology/2010/jan/08/stuart-jeffries-camera-phones

[13] http://www.telecomsmarketresearch.com/research/TMAAAPSF-Mobile-

Entertainment-Futures-2009-2013.shtml

[14] http://digital-photography-school.com/how-to-use-a-camera-phone

[15] C.H. Lee, T.C. Shen, L.Y. Liao, C.W. Chen, Y.P. Huang, and H.P. D. Shieh, "Multi-Electrically Driven Cylindrical Liquid Crystal Lens", IDMC (2009)

[16] http://en.wikipedia.org/wiki/Liquid_crystal

[17] T. Scharf, "Polarized Light in Liquid Crystal and Polymers", Chapter 8, Wiley-Interscience (2007)

[18] D.K. Yang, and S.T. Wu, "Fundamentals of Liquid Crystal Devices", Chapter 1, Wiley (2006)

[19] T. Scharf, "Polarized Light in Liquid Crystal and Polymers", Chapter 9, Wiley-Interscience (2007)

[20] D.K. Yang, and S.T. Wu, "Fundamentals of Liquid Crystal Devices", Chapter 12, Wiley (2006)

[21] A. Yariv, and P. Yeh, "Optical Waves in Crystal", Chapter 4, Wiley-Interscience (2003)

[22] J.W. Goodman, "Introduction to Fourier Optics", Chapter 4, New York: Mcgraw-Hill (2005)

[23] D.K. Yang, and S.T. Wu, "Fundamentals of Liquid Crystal Devices", Chapter 5, Wiley (2006)

[24] G.V. Vdovin, I.R. Gural'nik, S.P. Kotova, M.Yu. Lotkev, A.F. Naumov, "Liquid-crystal lenses with a controlled focal length. I. Theory", Quantum Electronics Vol. 29 p. 256-260 (1999)

[25] D. K. Cheng, "Field and Wave Electromagnetics", Chapter 9, Addison Wesley (1989)

[26] L.Y. Liao, P.Y. Shieh, and Y.P. Huang, "Marginal Electrode with Over-drive

Method for Fast Response Liquid Crystal Lens Applications", SID P-134 (2010)

[27] Y.M. Lin, L.Y. Liao, Y.P. Huang, and H.P. D. Shieh, "Tunable-Focus Cylindrical Liquid Crystal GRIN Lens Exhibiting Fast Response and Low Operating Voltage", TDC D-10 (2010)

[28] E. Hecht, "Optics", Addison Wesley, Chapter 11 (2002)

[29] http://www.normankoren.com/Tutorials/MTF.html

[30] J.W. Goodman, "Introduction to Fourier Optics", Chapter 6, New York: Mcgraw-Hill (2005)